G Porous Absorbers

If no extra reference is given in the sections of this chapter, see Mechel (1995).

The aims of the sections in this chapter are twofold: (1) derive the characteristic propagation constant Γ_a and the characteristic wave impedance Z_a of a plane wave in the porous material as functions of structure data and (2) derive the flow resistivity Ξ of the material as function of structure data because the flow resistivity is the most useful material parameter for the evaluation of Γ_a, Z_a. Different models of a porous material will be displayed; special attention will be given to fibrous materials. See also the sections about scattering in random media in the chapter "Scattering of Sound" for propagation constant and wave impedance in fibrous and granular media.

G.1   Structure Parameters of Porous Materials

The definition of structure parameters depends on the model theory in which they are applied (see the relevant sections for specific definitions). Especially, see the chapter about Biot's theory for special parameters of that theory. This section describes the structure parameters which come from the theory of the "quasi-homogeneous material" (see next section) because they are most often used to describe qualitatively porous absorber materials; the theory of the quasi-homogeneous material is the most simple theory.

Volume porosity σ_V, *massivity* μ:

The *volume porosity* σ_V is the ratio of air volume contained in the porous material to the total volume; it is given by $\sigma_V = 1 - \rho_a/\rho_m$ with ρ_a the bulk density of the porous absorber material and ρ_m the density of the (dense) matrix material. For glass or mineral fibre materials a value $\rho_m \approx 2250[\text{kg}/\text{m}^3]$ may be used.

For some considerations it is advantageous to apply the *massivity* $\mu = 1 - \sigma_V$.

The following table gives ranges of σ_V for some materials.

Structure factor χ :

The *structure factor* is the most ambiguous quantity in porous material theories. It is defined in the theory of the quasi-homogeneous material as $\chi = \sigma_V/\sigma_S$ with $\sigma_S = $ surface porosity of a cut through the material. Its value depends on the type of the pore shapes. The pore volume V_p is given by the integral of the pore surface S_p over a distance x normal to the considered pore surface:

$$V_p = \int_x S_p(x)\ dx \quad ; \quad \chi = \frac{\langle \sigma_S \rangle_x}{\sigma_S}. \tag{1}$$

Table 1 Ranges of porosity σ_v of some materials

Material	σ_v from	σ_v to
Mineral fibre materials	0.92	0.99
Foams	0.95	0.995
Felts	0.83	0.95
Wood-fibre board	0.65	0.80
Wood-wool board	0.50	0.65
Porous render	0.60	0.65
Pumice concrete	0.25	0.50
Pumice fill	0.65	0.85
Gravel and stone chip fill	0.25	0.45
Ceramic filtres	0.33	0.42
Brick	0.25	0.30
Sinter metal	0.10	0.25
Fire-clay	0.15	0.35
Sand stone	0.02	0.06
Marble		ca. 0.005

A model of an open-cellular foam consisting of cubic cells with connecting pores has the values:

$$\sigma_V \approx 1 - 3\frac{t}{d} \quad ; \quad \chi = \frac{(1 + \pi a/2)\,(d - 3t)}{\pi\,a^2}. \tag{2}$$

Two end corrections $\Delta\ell = \pi a/2$ have been added to the neck length t.
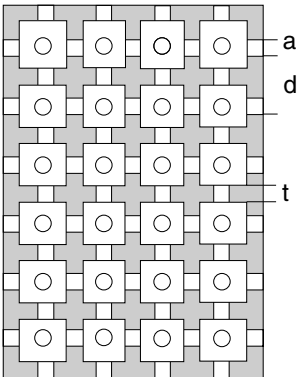
The following table gives the volume and surface porosities σ_V, σ_S and the structure factor χ of some regular model structures; a is the width of the pores, d is their distance.

Table 2 Porosities σ_V, σ_S and structure factor χ for regular models

Structure	σ_V	σ_S	χ
Flat pores, longitudinal or inclined	a/d	a/d	1
Square pores, longitudinal or inclined	$(a/d)^2$	$(a/d)^2$	1
Round pores, longitudinal or inclined	$\pi(a/d)^2/4$	$\pi(a/d)^2/4$	1
Square fibres, longitudinal or inclined	$2a/d - (a/d)^2$	$2a/d - (a/d)^2$	1
Round fibres, longitudinal or inclined	$1 - \pi(a/d)^2/4$	$1 - \pi(a/d)^2/4$	1
Square fibres, transversal	$2a/d - (a/d)^2$	a/d	$2 - a/d$
Round fibres, transversal	$1 - \pi(a/d)^2/4$	$1 - a/d$	$1 + a/d + (1 - \pi/4)(a/d)^2$
Array of cubes	$3a/d - 3(a/d)^2 + (a/d)^3$	$2a/d - (a/d)^2$	$3/2 - 3a/(4d) + (a/d)^2/8$

Flow resistivity Ξ; *absorber variable* E:

The *flow resistivity* Ξ of a porous material is its flow resistance per unit thickness for stationary flow with low velocity V (about V = 0.05 [cm/s]). For a material test sample of thickness dx:

$$\Xi = -\frac{1}{dx}\frac{dP}{V} \tag{3}$$

with dP the static pressure difference across the sample in flow direction.

Theories mostly determine the interior velocity V_i in a pore for a given pressure difference. This "internal" flow resistivity Ξ_i is related with the flow resistivity Ξ of the sample by $\Xi = \Xi_i/\sigma$.

A suitable non-dimensional quantity R is the ratio of the flow resistance $\Xi \cdot d$ of a layer of thickness d with the free field wave impedance Z_0: $R = \Xi \cdot d/Z_0$. According to

$$R = \frac{\Xi d}{\omega \rho_0 \cdot \lambda_0/2\pi}, \tag{4}$$

this is the ratio of the flow resistance to the mass reactance of a layer of air with thickness $\lambda_0/2\pi$. An important non-dimensional quantity for the evaluation of the characteristic data Γ_a, Z_a is the *absorber variable* (f = frequency):

$$E = \frac{\rho_0 f}{\Xi}. \tag{5}$$

One distinguishes with fibrous materials consisting of parallel fibres the flow resistivity$\Xi_\parallel$ if the flow is parallel to the fibres and $\Xi_\perp$ if the flow is transversal to the fibres. Empirical data by Sullivan for parallel fibre materials with mono-valued fibre radii a follow the relations:

$$\Xi_\parallel = 3.94 \cdot \frac{\eta}{a^2} \frac{\mu^{1.413}}{1-\mu} \left(1 + 27\,\mu^3\right) \tag{6}$$

and

$$\Xi_\perp = \begin{cases} 10.56\,\dfrac{\eta}{a^2}\,\dfrac{\mu^{1.531}}{(1-\mu)^3} & ; \quad a \approx 6 - 10\ [\mu m]\,, \\[3mm] 6.8\,\dfrac{\eta}{a^2}\,\dfrac{\mu^{1.296}}{(1-\mu)^3} & ; \quad a \approx 20 - 30\ [\mu m]. \end{cases} \tag{7}$$

---

a	= fibre radius;
η	= dynamic viscosity;
μ	= $1 - \sigma$ = massivity

Semi-empirical data (analytical relation fitted to experimental values) for fibre materials with mono-valued fibre radii a and random fibre orientation give:

$$\Xi = 4 \cdot \frac{\eta}{a^2} \left[0.55 \frac{\mu^{4/3}}{(1-\mu)} + \sqrt{2}\frac{\mu^2}{(1-\mu)^3}\right]. \tag{8}$$

Empirical data for fibrous materials with random fibre radius distribution and random fibre orientation can be approximated by:

$$\Xi = \frac{\eta}{\langle a^2 \rangle} \cdot \begin{cases} 3.2\ \mu^{1.42} & ; \text{ glass fiber material}\,, \\ 4.4\ \mu^{1.59} & ; \text{ mineral fiber material}. \end{cases} \tag{9}$$

G.2   Theory of the Quasi-homogeneous Material

An equivalent network is designed for a homogeneous material, taking into account a finite volume porosity σ_V, a structure factor χ of randomly oriented pores and a relaxation time constant τ for heat exchange between air and matrix material. A possible vibration of the matrix, induced by the friction between air and matrix, can also be included.
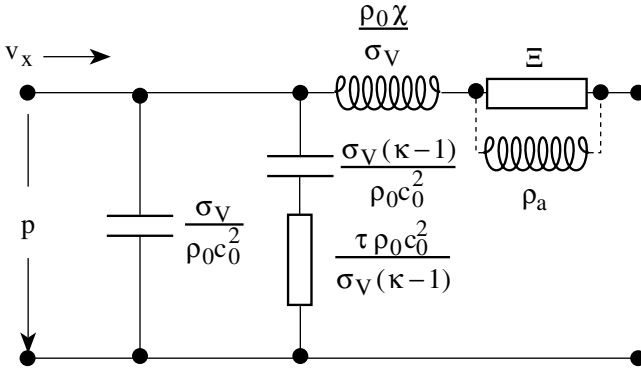
Equivalent network for unit length of a porous material

The first transversal branch represents the compressibility of the air in the material; the second transversal branch represents the relaxation due to heat exchange with the matrix; the first longitudinal element represents the inertia of the air in the pores (modified by the structure factor χ); the second longitudinal element represents the friction. If matrix vibration is included, the bulk density ρ_a of the material is parallel to Ξ. This can be taken into account by an effective resistivity:

$$\Xi \;\rightarrow\; \Xi_{\text{eff}} = \frac{j\omega\rho_a \cdot \Xi}{j\omega\rho_a + \Xi}. \tag{1}$$

Characteristic values:

$$\frac{\Gamma_a}{k_0} = j\sqrt{\chi\left(1 + \frac{\kappa - 1}{1 + j\omega\tau}\right) \cdot \left(1 - j\frac{\sigma_v\Xi}{\omega\rho_0\chi}\right)}, \tag{2}$$

$$\frac{Z_a}{Z_0} = \frac{1}{\sigma_v}\sqrt{\chi\left(1 - j\frac{\sigma_v\Xi}{\omega\rho_0\chi}\right) \Big/ \left(1 + \frac{\kappa - 1}{1 + j\omega\tau}\right)}. \tag{3}$$

k_0	= free field wave number;
Z_0	= free field wave impedance;
ρ_0	= density of air;
ω	= angular frequency;
κ	= adiabatic exponent of air;
Ξ	= flow resistivity;
χ	= structure factor;
σ_v	= volume porosity;
τ	= heat relaxation time constant

Introducing $E = \rho_0 f / \Xi$ and $E_0 = \rho_0 f_0 / \Xi$ with $f_0 =$ relaxation frequency, the characteristic values are:

$$\frac{\Gamma_a}{k_0} = j \sqrt{\frac{\kappa + jE/E_0}{1 + jE/E_0}} \cdot \left(\chi - j\frac{\sigma_v}{2\pi E} \right) \quad ; \quad \frac{Z_a}{Z_0} = \frac{1}{\sigma_v} \sqrt{\frac{1 + jE/E_0}{\kappa + jE/E_0}} \cdot \left(\chi - j\frac{\sigma_v}{2\pi E} \right) . \quad (4)$$

$E_0 \to 0$ belongs to an isothermal sound wave in the material; $E_0 \to \infty$ belongs to an adiabatic sound wave; $E_0 = 0.1$ is a typical value for mineral fibre materials.
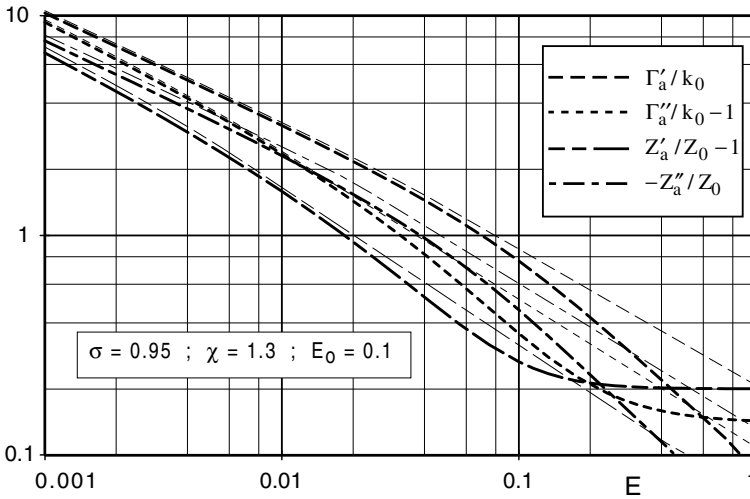
Thick lines: theory of quasi-homogeneous material; thin lines: measured values

G.3 Rayleigh Model with Round Capillaries

The Rayleigh model has for a long time been the only existing model for porous materials.

This model consists of parallel circular capillaries with radius a and mutual distance d in a bloc of the matrix material. The sound propagation in the capillary is determined with viscous and thermal losses at the capillary wall taken into account. See ❯ *Ch. J*, "Duct Acoustics", for sound propagation in capillaries. The arrangement and mutual distance of the capillaries is supposed to be such that a prescribed porosity σ is obtained (e.g. $\sigma = \pi a^2 / d^2$ for a square arrangement), even if the value of the porosity cannot be realised physically (in a square arrangement the realisable porosity is $\sigma \le \pi/4 = 0.785$), because only a single capillary is considered. The theory gives the propagation constant Γ_a of the density wave (which is considered to be the propagation constant of sound in the porous material) and the "interior" axial wave impedance Z_i of the density wave in a capillary. Its relation to the desired wave impedance Z_a of the porous material is $Z_a = Z_i / \sigma$.

The normalised characteristic values of a cell are:

$$\frac{\Gamma_a}{k_0} = j\sqrt{\frac{\rho_{eff}}{\rho_0} \cdot \frac{C_{eff}}{C_0}} \quad ; \quad \frac{Z_i}{Z_0} = \sqrt{\frac{\rho_{eff}}{\rho_0} \Big/ \frac{C_{eff}}{C_0}} \tag{1}$$

with the ratios of the effective air density and air compressibility (index 0 indicates free field values):

$$\frac{\rho_{eff}}{\rho_0} = \frac{1}{1 - J_{1,0}(k_\nu a)} \quad ; \quad \frac{C_{eff}}{C_0} = 1 + (\kappa - 1) \cdot J_{1,0}(k_{\alpha 0} a) \tag{2}$$

and the function

$$J_{1,0}(z) = 2\frac{J_1(z)}{z \cdot J_0(z)} = 2 \cdot \frac{1}{2-} \frac{z^2}{4-} \frac{z^2}{6-} \frac{z^2}{8-\ldots} \cdots \frac{z^2}{2 \cdot n - \ldots} \quad ; \quad n = 1,\ 2,\ 3 \ldots \tag{3}$$

with Bessel functions $J_n(z)$ and the continued-fraction expansion of their ratio in the last term (the expansion must go until $|z|^2/(2n) \ll 1$). The asymptotic approximation

$$J_{1,0}(z) \approx \frac{2}{z} \frac{\tan\left(z - \frac{\pi}{4}\right) + \frac{3}{8z}}{1 + \frac{1}{8z} \tan\left(z - \frac{\pi}{4}\right)} \tag{4}$$

may be applied for large arguments $|z|$.

The squares of the used wave numbers are:

$$k_\nu^2 = -j\omega/\nu \quad ; \quad k_{\alpha 0}^2 = k_\nu^2 \cdot \sqrt{\kappa\, \text{Pr}}. \tag{5}$$

κ	=	adiabatic exponent;
ν	=	kinematic viscosity;
η	=	dynamic viscosity;
Pr	=	Prandtl number;
μ	=	cell massivity;
C_0	=	$1/(\rho_0 c_0^2)$;
Ξ	=	flow resistivity

The argument $k_\nu a$ should be replaced with an argument which can be applied also for material with random pore radius distribution. This is the "absorber variable" $E = \rho_0 f / \Xi$. For its application, the flow resistivity Ξ_i in a pore must be determined.

The flow velocity profile in a circular capillary is, with the static pressure gradient dP/dx:

$$V(r) = -\frac{1}{4\eta} \frac{dP}{dx} (a^2 - r^2). \tag{6}$$

The flow resistivity Ξ_i is defined with the volume flow Q through the capillary cross-section area S:

$$\Xi_i = \frac{-dP/dx \cdot S}{Q} = \frac{8\eta}{a^2} \quad ; \quad Q = -\frac{\pi a^4}{8\eta} \frac{dP}{dx}. \tag{7}$$

Thus the desired relations between the arguments are:

$$(k_v a)^2 = -16\pi j\, E \quad ; \quad (k_{\alpha 0} a)^2 = -16\pi j\, \kappa\, Pr\ E. \tag{8}$$

If in a material test the (exterior) flow resistivity Ξ is determined, its relation to the interior flow resistivity is $\Xi = \Xi_i/\sigma$ with the porosity σ of the material.

The continued-fraction approximation (up to the fifth fraction) of the characteristic values is with the variable E:

$$\left(\frac{\Gamma_i}{k_0}\right)^2 = -\kappa \frac{75 + 30\pi j\, [8 + Pr(5 + 3\kappa)]\, E - \pi^2[90 + Pr(480 + 288\kappa) + \ldots}{2\pi E\,\{75j - 40\pi(1 + 6\kappa\, Pr)\, E - \ldots}$$

$$\frac{+ Pr^2\, \kappa(80 + 10\kappa)]\, E^2 - 4\pi^3 j\, Pr[45 + 27\kappa + \kappa\, Pr(84 + 8\kappa)]\, E^3 + \ldots}{-2\pi^2 j\,\kappa\, Pr(64 + 45\kappa\, Pr)\, E^2 + \ldots} \tag{9}$$

$$\frac{+12\pi^4\kappa\, Pr^2(8 + \kappa)\, E^4}{+48\pi^3(\kappa\, Pr)^2\, E^3\}},$$

$$\left(\frac{Z_i}{Z_0}\right)^2 = \frac{1}{\kappa}\, \frac{225 + 720\pi j\, (1 + \kappa\, Pr)\, E - 18\pi^2[15 + \ldots}{2\pi E\,\{225j - 30\pi[4 + Pr(15 + 9\kappa)]\, E - 6\pi^2 j\ Pr[40 + 24\kappa + \ldots} \tag{10}$$

$$\frac{+\kappa\, Pr(128 + 15\kappa\, Pr)]E^2 - 864\pi^3 jk\, Pr(1 + \kappa\, Pr)\, E^3 + 324\pi^4(\kappa\, Pr)^2\, E^4}{+\kappa\, Pr(40 + 5\kappa)]\, E^2 + 16\pi^3\kappa\, Pr^2(8 + \kappa)\, E^3\}}.$$
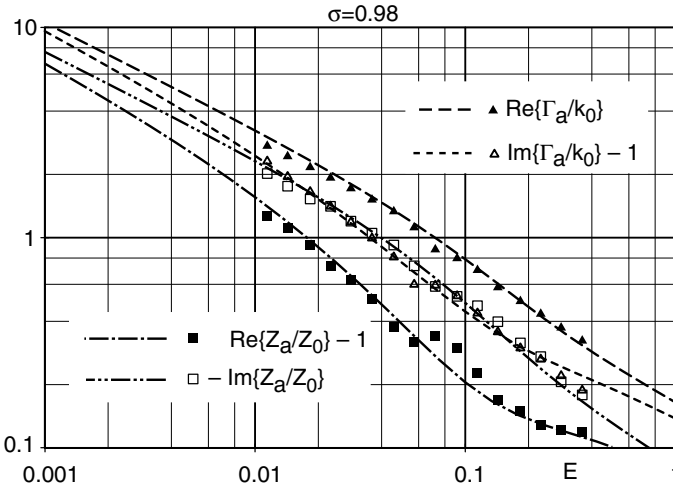
Comparison of the characteristic values from the Rayleigh model (curves) with measurements at a technical mineral fibre absorber (points)

G.4   Model with Flat Capillaries

The good agreement between characteristic values from measurements with fibrous absorber materials and the theory of the Rayleigh model is rather surprising because

the Rayleigh model has a somehow "inverted" geometry as compared to a fibre material. Therefore the simpler model with flat capillaries (instead of round capillaries) may have a chance, also.

The model consists of parallel flat capillaries, 2h wide and in a mutual distance d, in a bloc of the matrix material. The sound propagation in the capillary is determined with viscous and thermal losses at the capillary walls taken into account. See ❯ *Sects. J.1 and J.2 in Ch. J*, "Duct Acoustics", for sound propagation in capillaries. The arrangement and mutual distance of the capillaries is supposed to be such that a prescribed porosity σ is obtained (σ = 2h/d). The theory gives the propagation constant Γ_a of the density wave (which is considered to be the propagation constant of sound in the porous material), and the "interior" axial wave impedance Z_i of the density wave in a capillary. Its relation to the wanted wave impedance Z_a of the porous material is $Z_a = Z_i/\sigma$.

The normalised characteristic values of a capillary are:

$$\frac{\Gamma_a}{k_0} = j\sqrt{\frac{\rho_{eff}}{\rho_0} \cdot \frac{C_{eff}}{C_0}} \quad ; \quad \frac{Z_i}{Z_0} = \sqrt{\frac{\rho_{eff}}{\rho_0} \Big/ \frac{C_{eff}}{C_0}} \tag{1}$$

with the ratios of the effective air density and air compressibility (index 0 indicates free field values):

$$\frac{\rho_{eff}}{\rho_0} = \frac{1}{1 - \dfrac{\tan(k_\nu h)}{k_\nu h}} \quad ; \quad \frac{C_{eff}}{C_0} = 1 + (\kappa - 1)\frac{\tan(k_{\alpha 0} h)}{k_{\alpha 0} h}. \tag{2}$$

The squares of the used wave numbers are:

$$k_\nu^2 = -j\,\omega/\nu \quad ; \quad k_{\alpha 0}^2 = k_\nu^2 \cdot \kappa\,Pr. \tag{3}$$

κ	=	adiabatic exponent;
ν	=	kinematic viscosity;
η	=	dynamic viscosity;
Pr	=	Prandtl number;
C_0	=	$1/(\rho_0 c_0^2)$;
Ξ	=	flow resistivity

The argument $k_\nu h$ should be replaced with an argument which can be applied also for material with random pore width distribution. This is the "absorber variable" $E = \rho_0 f / \Xi$. For its application, the flow resistivity Ξ_i in a pore must be determined.

The flow velocity profile in a flat capillary is, with the static pressure gradient dP/dx and y the transversal co-ordinate:

$$V(y) = -\frac{1}{2\eta}\frac{dP}{dx}(h^2 - y^2). \tag{4}$$

The flow resistivity Ξ_i is defined with the volume flow Q through the capillary cross-section:

$$\Xi_i = \frac{-dP/dx \cdot 2h}{Q} = \frac{3\eta}{h^2} \quad ; \quad Q = 2\int_0^h V(y)dy = -\frac{2}{3\eta}\frac{dP}{dx}h^3. \tag{5}$$

Thus the wanted relations between the arguments are:

$$|k_v h|^2 = 6\pi E \quad ; \quad (k_v h)^2 = -6\pi j\ E \quad ; \quad (k_{\alpha 0}h)^2 = -6\pi j\ \kappa\ Pr\ E. \tag{6}$$

If in a material test the (exterior) flow resistivity Ξ is determined, its relation to the interior flow resistivity is $\Xi = \Xi_i/\sigma$ with the porosity σ of the material.
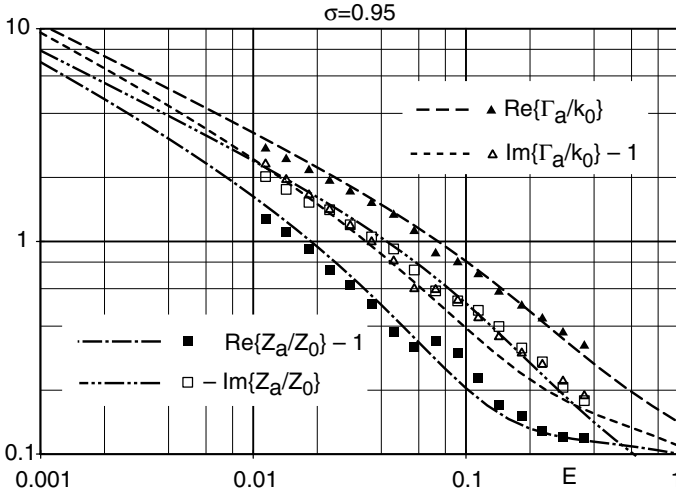
Comparison of the characteristic values from the model with flat capillaries (curves) with measurements at a technical mineral fibre absorber (points)

G.5   Longitudinal Flow Resistivity in Parallel Fibres

The geometry of the fibre bundle models agrees better with the geometry of real fibrous materials. First a regular arrangement of the fibres is used in the theory, then the diameters and distances of the fibres are randomised. The direction of flow and sound relative to the fibres must be treated separately, when it is parallel to the fibres or transversal.
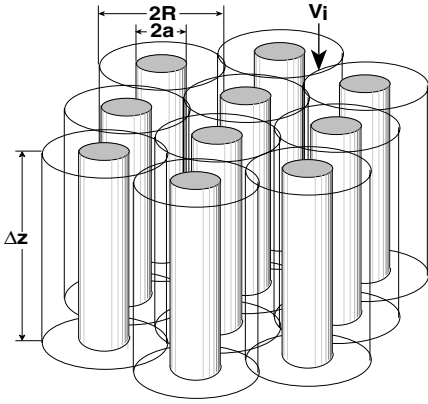
Regular arrangement:

Fibres of equal radius a are arranged in a regular array with cells of radius R around each fibre. The flow velocity V_i is *parallel* to the fibres.

The cell radius R is adjusted to give the porosity σ:

$$\sigma = 1 - (a/R)^2 = 1 - N \cdot \pi a^2 \quad \text{with N = number of fibres in unit area.} \tag{1}$$

Velocity profile of viscous flow in a cell (with C = a free factor; z axis in flow direction):

$$v_z(r) = C \left[\frac{R^2}{2} \ \ln \ \frac{r}{a} - \frac{1}{4} \ (r^2 - a^2) \right]. \tag{2}$$

Flow resistivity, with definition $\quad \Xi_{\parallel} = (-\partial p/\partial z) \big/ \langle v_z \rangle$: $\tag{3}$

$$\Xi_{\parallel} = (-\partial p/\partial z) \big/ \langle v_z \rangle = \frac{4\eta}{a^2} \ \frac{\mu}{2\mu - \ln \ \mu - \frac{1}{2}\mu^2 - 1,5} \tag{4}$$

with η = dynamic viscosity of air; $\mu = 1 - \sigma$ = massivity.

Random arrangement:

A material sample contains I cells, $i = 1, 2, \ldots,$ I with random variation of the fibre radius a_i and/or the cell cross-section area $S_i = \pi R_i^2$, which gives a massivity $\mu_i = (a_i/R_i)^2$ of each cell. The resulting flow resistivity is:

$$\Xi_{\parallel} = \frac{4\eta}{\sum\limits_{i=1}^{I} R_i^2 \cdot \dfrac{S_i}{\sum\limits_{i} S_i} \cdot (2\,\mu_i - 0,5\,\mu_i^2 - \ln \ \mu_i - 1,5)}. \tag{5}$$

One can collect the fibre radii a_i in groups around radius group values a_m with a relative frequency q_m and correspondingly the cell radii R_i in groups around group radii R_n with relative frequency p_n. The flow resistivity is:

$$\Xi_{\parallel} = \frac{4\eta \ \ <a_m^2> }{\mu \ \sum\limits_{m,n} q_m \, p_n \cdot R_n^4 \left[2 \left(\dfrac{a_m}{R_n} \right)^2 - \dfrac{1}{2} \left(\dfrac{a_m}{R_n} \right)^4 - 2 \ \ln \ \left(\dfrac{a_m}{R_n} \right) - 1,5 \right]}. \tag{6}$$

Technical fibrous absorbers mostly have Poisson distributions of the a_m and R_n.

G.6   Longitudinal Sound in Parallel Fibres

Suppose a fibre model as in ⦿ *Sect. G.4* with sound propagation parallel to the fibres.

The sound field in each cell is evaluated with viscous and thermal losses (at the isothermal fibre surface) taken into account. The propagation constant of the density wave is Γ_a; the axial wave impedance of the density wave is Z_i (interior wave impedance); its relation to the characteristic impedance Z_a (exterior wave impedance) of a material sample is $Z_a = Z_i/\sigma$, with σ = porosity of the material.

The normalised characteristic values of a cell are:

$$\frac{\Gamma_a}{k_0} = j\sqrt{\frac{\rho_{\text{eff}}}{\rho_0} \cdot \frac{C_{\text{eff}}}{C_0}} \quad ; \quad \frac{Z_i}{Z_0} = \sqrt{\frac{\rho_{\text{eff}}}{\rho_0} \Big/ \frac{C_{\text{eff}}}{C_0}} \tag{1}$$

with the ratios of the effective air density and air compressibility (index 0 indicates free field values):

$$\frac{\rho_{\text{eff}}}{\rho_0} = \frac{1}{1 - H_{1,0}(k_\nu a\,;\,\mu)} \quad ; \quad \frac{C_{\text{eff}}}{C_0} = 1 + (\kappa - 1) \cdot H_{1,0}(k_{\alpha,0}a\,;\,\mu) \tag{2}$$

and the function

$$H_{1,0}(x, \mu) = \frac{-2\,\mu}{x\,(1 - \mu)} \frac{J_1(x/\sqrt{\mu}) \cdot Y_1(x) - J_1(x) \cdot Y_1(x/\sqrt{\mu})}{J_1(x/\sqrt{\mu}) \cdot Y_0(x) - J_0(x) \cdot Y_1(x/\sqrt{\mu})} \tag{3}$$

with Bessel functions $J_n(z)$ and Neumann functions $Y_n(z)$. The squares of the used wave numbers are $k_\nu^2 = -j\,\omega/\nu \quad ; \quad k_{\alpha 0}^2 = k_\nu^2 \cdot \sqrt{\kappa\,\Pr}$. $\tag{4}$

κ = adiabatic exponent;
ν = kinematic viscosity;
$\Pr$ = Prandtl number;
μ = cell massivity;
$C_0 = 1/(\rho_0 c_0^2)$

The replacement of the argument $k_\nu a$ with the absorber variable $E = \rho_0 f / \Xi$ is performed with the result of the previous ⦿ *Sect. G.5*:

$$E = \frac{1}{8\pi} |k_\nu a|^2 \frac{2\mu - \ln\mu - \frac{1}{2}\mu^2 - 1.5}{\mu} \approx \frac{1}{8\pi} |k_\nu a|^2 \frac{2\mu - \ln\mu - 1.5}{\mu}, \tag{5}$$

$$|k_\nu a|^2 = 8\pi\,E \frac{\mu}{2\mu - \ln\mu - \frac{1}{2}\mu^2 - 1.5} \approx 8\pi\,E \frac{\mu}{2\mu - \ln\mu - 1.5}. \tag{6}$$

The present model also permits one to determine the relaxation (angular) frequency ω_0 of the heat transfer between sound wave and matrix (ω_0 was needed in ⦿ *Sect. G.2*, but it was not possible there to determine its magnitude). The relaxation is marked by a

deep minimum of $\mathrm{Im}\{C_{\mathrm{eff}}/C_0\}$ in the plane of $|k_\nu a|^2$ and massivity μ. Its position gives the relations:

$$|k_\nu a|^2 = \frac{\omega_0}{\nu}a^2 = 10^{(1.69843 + 2.58454\ \log\mu + 0.541408\ (\log\mu)^2 + 0.0726279\ (\log\mu)^3)},$$

$$(7)$$

$$\omega_0 = \frac{\nu}{a^2}\,|k_\nu a|^2 = \frac{\nu}{a^2}\cdot 10^{(1.69843 + 2.58454\ \log\mu + 0.541408\ (\log\mu)^2 + 0.0726279\ (\log\mu)^3)}.$$
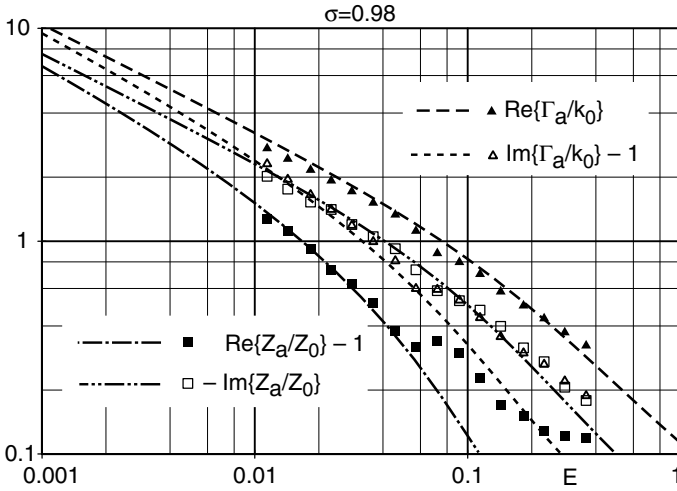
Comparison of the characteristic values from the model of a regular arrangement of longitudinal fibres (curves) with measured data from a technical mineral fibre absorber

The model of parallel fibres with longitudinal sound propagation can be easily randomised with respect to the fibre radii a_i and cell radii R_i or cell areas $A_i = \pi R_i^2$. Their random values are counted in groups of interval widths Δa, ΔA around average group values a_m, A_n. If their relative frequencies q_m, p_n have the forms of Poisson distributions with distribution parameters λ, Λ

$$q_m = e^{-\lambda}\frac{\lambda^m}{m!}\quad;\quad p_n = e^{-\Lambda}\frac{\Lambda^n}{n!}\quad;\quad m,\ n = 0,\ 1,\ 2,\ \ldots,$$

$$(8)$$

$$\left\langle a_m^2\right\rangle = (\lambda^2 + 2\lambda + 1/4)\,\Delta a^2\quad;\quad \langle A_n\rangle = (\Lambda + 1/2)\,\Delta A$$

with the total and the group massivities

$$\mu = \pi\frac{<a_m^2>}{<A_n>}\quad;\quad \mu_{mn} = \mu\,\frac{\Lambda + 1/2}{\lambda^2 + 2\lambda + 1/4}\,\frac{(m + 1/2)^2}{n + 1/2},$$

$$(9)$$

the effective group densities and compressibilities are:

$$\frac{\rho_{mn}}{\rho_0} = \frac{1}{1 - H_{1,0}(k_\nu a_m\,,\ \mu_{mn})}\quad;\quad \frac{C_{mn}}{C_0} = 1 + (\kappa - 1)\,H_{1,0}(k_{\alpha 0}a_m\,,\ \mu_{mn}).$$

$$(10)$$

The characteristic values are evaluated from the statistically relevant density ρ_s and compressibility C_s by:

$$\frac{\Gamma_a}{k_0} = j\sqrt{\frac{\rho_s}{\rho_0} \cdot \frac{C_s}{C_0}} \quad ; \quad \frac{Z_i}{Z_0} = \sqrt{\frac{\rho_s}{\rho_0} \Big/ \frac{C_s}{C_0}} \tag{11}$$

with

$$1\Big/\frac{\rho_s}{\rho_0} = \frac{\overset{<}{\underset{m,n}{\sum}} q_m\, p_n \Big/ \frac{\rho_{mn}}{\rho_0}}{\underset{m,n}{\overset{<}{\sum}} q_m\, p_n} \quad ; \quad \frac{C_s}{C_0} = \frac{\overset{<}{\underset{m,n}{\sum}} q_m\, p_n \frac{C_{mn}}{C_0}}{\underset{m,n}{\overset{<}{\sum}} q_m\, p_n}, \tag{12}$$

where the upper symbol $<$ at the summation sign indicates that the summation is performed only if $\mu_{mn} < 1$; otherwise it is skipped. Typical values of the distribution parameters are $\lambda = 2.5$ (deviations thereof have little influence on the result) and $\Lambda = 4.5$.
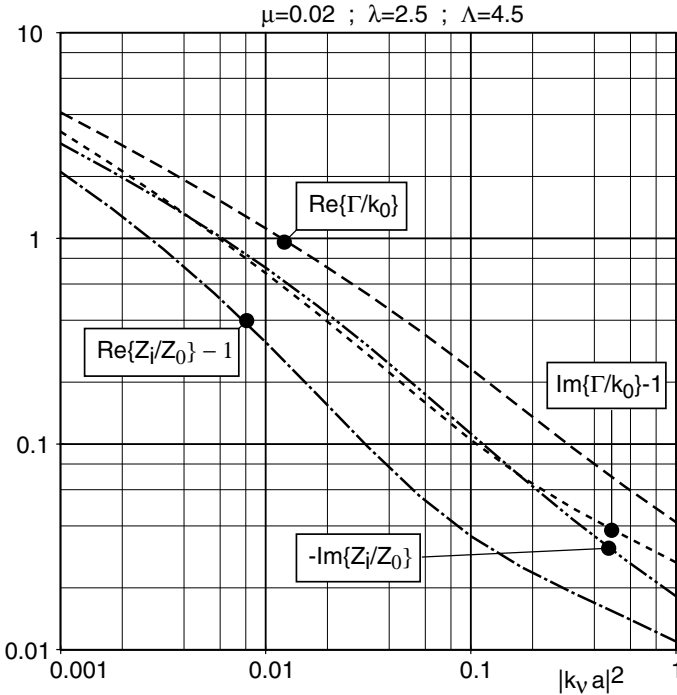

Characteristic values from model with parallel fibres and longitudinal sound propagation if the fibre radii and the cell radii are Poisson distributed

G.7   Transversal Flow Resistivity in Parallel Fibres

The model is as depicted in ▶ *Sect. G.5*, but the flow velocity V_i is normal to the fibres. Analytical studies (see Mechel, 1995) have shown that a cell model, in which the cell

"walls" are immaterial symmetry surfaces for the disturbance flow field (u, v), can be used also for this transversal flow as an approximation (in fact there is a windward-to-lee unbalance, but it is small for massivity values as they are found for technical fibre absorbers).

The cell and the incoming flow U are as in the sketch. The flow field is $\vec{V} = U \cdot (1 + u, \ v)$. The disturbance flow $\vec{v}$ and its radial derivative are supposed to be zero on the cell surface. Besides the Cartesian co-ordinates (x, y), also cylindrical co-ordinates (r, φ) are used ($\varphi = 0$ on the x axis).
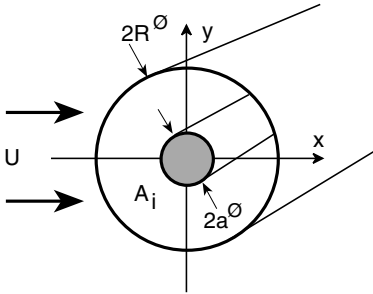
General solutions with the present conditions of symmetry of the Navier–Stokes equation are:

$$u(kr, \varphi) = \vec{v}_x / U$$

$$= -\frac{C_0 \ \cos \varphi}{kr} - \sum_{m \geq 1} m \ [C_m \ (kr)^{m-1} \cdot \cos(m-1)\varphi - D_m \ (kr)^{-m-1}$$

$$\cdot \cos(m+1)\varphi] - \frac{1}{2} e^{kr \ \cos \varphi} \cdot \sum_{n \geq 0} A_n \cdot [(\cos n\varphi + \frac{n}{kr} \cos(n+1)\varphi) \tag{1}$$

$$\cdot I_n(kr) - \cos \varphi \ \cos n\varphi \ I_{n-1}(kr)]$$

$$+ B_n \cdot [(\cos n\varphi + \frac{n}{kr} \cos(n+1)\varphi) \ K_n(kr) - \cos \varphi \ \cos n\varphi \ K_{n-1}(kr)],$$

$$v(kr, \varphi) = \vec{v}_y / U$$

$$= -\frac{C_0 \ \sin \varphi}{kr} - \sum_{m \geq 1} m \ [C_m \ (kr)^{m-1} \cdot \sin(m-1)\varphi + D_m \ (kr)^{-m-1}$$

$$\cdot \sin(m+1)\varphi] - \frac{1}{2} e^{kr \ \cos \varphi} \cdot \sum_{n \geq 0} A_n \cdot [\frac{n}{kr} \sin(n+1)\varphi \tag{2}$$

$$\cdot I_n(kr) - \sin \varphi \ \cos n\varphi \ I_{n-1}(kr)]$$

$$+ B_n \cdot [\frac{n}{kr} \sin(n+1)\varphi) \ K_n(kr) + \sin \varphi \ \cos n\varphi \ K_{n-1}(kr)]$$

with the flow parameter $k = U/(2\nu)$ (ν = kinematic viscosity), the modified Bessel functions $I_m(z)$, $K_m(z)$ of the first and second kind, and yet undetermined coefficients A_n, B_n, C_n, D_n. These are determined from the boundary conditions

$$u(ka, \varphi)\big|_{kr=ka} = -1 \quad ; \quad v(ka, \varphi)\big|_{kr=ka} = 0 \quad ;$$

$$u_r(kr, \varphi)\big|_{kr=kR} = 0 \quad ; \quad \frac{\partial u_\varphi(kr, \varphi)}{\partial kr}\bigg|_{kr=kR} = 0, \tag{3}$$

which, with a summation up to m, n = 3, gives a linear system of equations of the following form:

$$\begin{bmatrix} c_{1,1} & c_{1,2} & \cdots & c_{1,14} & c_{1,15} \\ c_{2,1} & c_{2,2} & \cdots & c_{2,14} & c_{2,15} \\ \vdots & \vdots & & \vdots & \vdots \\ c_{15,1} & c_{15,2} & \cdots & c_{15,14} & c_{15,15} \end{bmatrix} \cdot \begin{bmatrix} A_0 \\ A_1 \\ \vdots \\ D_3 \end{bmatrix} = \begin{bmatrix} -1 \\ 0 \\ \vdots \\ 0 \end{bmatrix} \tag{4}$$

with the list of unknown coefficients

$$\{A_0, A_1, A_2, A_3, B_0, B_1, B_2, B_3, C_0, C_1, C_2, C_3, D_1, D_2, D_3, \} \tag{5}$$

and the matrix coefficient rows $c_i = \{c_{i1}, c_{i2}, c_{i3}, \ldots, c_{i15}\}$: $\tag{6}$

$$\begin{aligned}
c_1 = \{ & -(1/2 + ka^2/8) \cdot I_0(ka) + (ka/4 + ka^3/32) \cdot I_1(ka), \\
& (1/4 + 3ka^2/32) \cdot I_0(ka) - (5ka/16 + ka^3/32) \cdot I_1(ka), \\
& (ka/8 + ka^3/48) \cdot I_1(ka) - ka^2/12 \cdot I_2(ka), \\
& ka^2/32 \cdot I_2(ka) - ka^3/96 \cdot I_3(ka), \\
& -(1/2 + ka^2/8) \cdot K_0(ka) - (ka/4 + ka^3/32) \cdot K_1(ka), \\
& -(1/4 + 3ka^2/32) \cdot K_0(ka) - (5ka/16 + ka^3/32) \cdot K_1(ka), \\
& -(ka/8 + ka^3/48) \cdot K_1(ka) - ka^2/12 \cdot K_2(ka), \\
& -ka^2/32 \cdot K_2(ka) - ka^3/96 \cdot K_3(ka), \\
& 0, -1, 0, 0, 0, 0, 0\};
\end{aligned}$$

$$\begin{aligned}
c_2 = \{ & -(ka/2 + ka^3/16) \cdot I_0(ka) + (1/2 + 3ka^2/16) \cdot I_1(ka), \\
& (3ka/8 + 5ka^3/96) \cdot I_0(ka) - (3/4 + 11ka^2/48) \cdot I_1(ka), \\
& (1/4 + ka^2/8) \cdot I_1(ka) - (3ka/8 + ka^3 24) \cdot I_2(ka), \\
& (ka/8 + 5ka^3/192) \cdot I_2(ka) - 3ka^2/32 \cdot I_3(ka), \\
& -(ka/2 + ka^3/16) \cdot K_0(ka) - (1/2 + 3ka^2/16) \cdot K_1(ka), \\
& -(3ka/8 + 5ka^3/96) \cdot K_0(ka) + (-3/4 - 11ka^2/48) \cdot K_1(ka), \\
& (-1/4 - ka^2/8) \cdot K_1(ka) - (3ka/8 + ka^3/24) \cdot K_2(ka), \\
& -(ka/8 + 5ka^3/192) \cdot K_2(ka) - 3ka^2/32 \cdot K_3(ka), \\
& -1/ka, 0, -2ka, 0, 0, 0, 0\};
\end{aligned}$$

$c_3 = \{ - ka^2/8 \cdot I_0(ka) + (ka/4 + ka^3/24) \cdot I_1(ka),$

$\quad (1/4 + ka^2/8) \cdot I_0(ka) - (1/(2ka) + 3ka/8 - ka^3/24) \cdot I_1(ka),$

$\quad (ka/4 + 7ka3/192) \cdot I_1(ka) - (1 + 3ka^2/16) \cdot I_2(ka),$

$\quad (1/4 + 3ka^2/32) \cdot I_2(ka) - (7ka/16 + ka^3/32) \cdot I_3(ka),$

$\quad -ka^2/8 \cdot K_0(ka) + (-ka/4 - ka^3/24) \cdot K_1(ka),$

$\quad -(-1/4\,ka^2/8) \cdot K_0(ka) - (1/(2ka) + 3ka/8 + ka^3/24) \cdot K_1(ka),$

$\quad -(ka/4 + 7ka^3/192) \cdot K_1(ka) - (1 + 3ka^2/16) \cdot K_2(ka),$

$\quad -(1/4 + 3ka^2/32) \cdot K_2(ka) - (7ka/16 + ka^3/32) \cdot K_3(ka),$

$\quad 0, 0, 0, -3ka^2, ka^{-2}, 0, 0\};$

$c_4 = \{ - ka^3/48 \cdot I_0(ka) + ka^2/16 \cdot I_1(ka),$

$\quad (ka/8 + 5ka^3/192) \cdot I_0(ka) - (1/4 + 3ka^2/32) \cdot I_1(ka),$

$\quad (1/4 + 3ka^2/32) \cdot I_1(ka) - (ka^{-1} + ka/2 + ka^3/32) \cdot I_2(ka),$

$\quad (ka/4 + ka^3/32) \cdot I_2(ka) - (5/4 + 7ka^2/32) \cdot I_3(ka),$

$\quad -ka^3/48 \cdot K_0(ka) - ka^2/16 \cdot K_1(ka),$

$\quad -(ka/8 + 5ka^3/192) \cdot K_0(ka) - (1/4 + 3ka^2/32) \cdot K_1(ka),$

$\quad -(1/4 + 3ka^2/32) \cdot K_1(ka) - (ka^{-1} + ka/2 + ka^3/32) \cdot K_2(ka),$

$\quad -(ka/4 + ka^3/32) \cdot K_2(ka) - (5/4 + 7ka^2/32) \cdot K_3(ka),$

$\quad 0, 0, 0, 0, 0, 2/ka^3, 0\};$

$c_5 = \{ka^3/96 \cdot I_1(ka),$

$\quad ka^2/32 \cdot I_0(ka) - (ka/16 + ka^3/96) \cdot I_1(ka),$

$\quad (ka/8 + ka^3/48) \cdot I_1(ka) - (1/2 + ka^2/8) \cdot I_2(ka),$

$\quad (1/4 + 3ka^2/32) \cdot I_2(ka) - (3/(2ka) + 5ka/8 + ka^3/32) \cdot I_3(ka),$

$\quad -ka^3/96 \cdot K_1(ka),$

$\quad -ka^2/32 \cdot K_0(ka) - (ka/16 + ka^3/96) \cdot K_1(ka),$

$\quad -(ka/8 + ka^3/48) \cdot K_1(ka) - (1/2 + ka^2/8) \cdot K_2(ka),$

$\quad -(1/4 + 3ka^2/32) \cdot K_2(ka) - (3/(2ka) + 5ka/8 + ka^3/32) \cdot K_3(ka),$

$\quad 0, 0, 0, 0, 0, 0, 3/ka^4\};$

$c_6 = \{(1/2 + ka^2/16) \cdot I_1(ka),$

$\quad (ka/8 + ka^3/96) \cdot I_0(ka) - (1/4 + ka^2/48) \cdot I_1(ka),$

$\quad -I_1(ka)/4 - ka/8 \cdot I_2(ka),$

$\quad -(ka/8 + ka^3/192) \cdot I_2(ka) - ka^2/32 \cdot I_3(ka),$

$\quad -(1/2 + ka^2/16) \cdot K_1(ka),$

$\quad -(ka/8 + ka^3/96) \cdot K_0(ka) - (1/4 + ka^2/48) \cdot K_1(ka),$

$\quad K_1(ka)/4 - ka/8 \cdot K_2(ka),$

$\quad (ka/8 + ka^3/192) \cdot K_2(ka) - ka^2/32 \cdot K_3(ka),$

$\quad -1/ka, 0, 2ka, 0, 0, 0, 0\};$

$c_7 = \{(ka/4 + ka^3/48) \cdot I_1(ka),$

$\quad (1/4 + ka^2/16) \cdot I_0(ka) - (1/(2ka) + ka/8) \cdot I_1(ka),$

$\quad ka^3/192 \cdot I_1(ka) - (1/2 + ka^2/16) \cdot I_2(ka),$

$\quad -(1/4 + ka^2/32) \cdot I_2(ka) - 3ka/16 \cdot I_3(ka),$

$\quad -(ka/4 + ka^3/48) \cdot K_1(ka),$

$\quad -(1/4 + ka^2/16) \cdot K_0(ka) - (1/(2ka) + ka/8) \cdot K_1(ka),$

$\quad -ka^3/192 \cdot K_1(ka) - (1/2 + ka^2/16) \cdot K_2(ka),$

$\quad (1/4 + ka^2/32) \cdot K_2(ka) - 3ka/16 \cdot K_3(ka),$

$\quad 0, 0, 0, 3ka^2, 1/ka^2, 0, 0\};$

$c_8 = \{ka^2/16 \cdot I_1(ka),$

$\quad (ka/8 + ka^3/64) \cdot I_0(ka) - (1/4 + ka^2/32) \cdot I_1(ka),$

$\quad (1/4 + ka^2/32) \cdot I_1(ka) - (1/ka + ka/4) \cdot I_2(ka),$

$\quad -(3/4 + 3ka^2/32) \cdot I_3(ka),$

$\quad -ka^2/16 \cdot K_1(ka),$

$\quad -(ka/8 + ka^3/64) \cdot K_0(ka) - (1/4 + ka^2/32) \cdot K_1(ka),$

$\quad -(1/4 + ka^2/32) \cdot K_1(ka) - (1/ka + ka/4) \cdot K_2(ka),$

$\quad -(3/4 + 3ka^2/32) \cdot K_3(ka),$

$\quad 0, 0, 0, 0, 0, 2/ka^3, 0\};$

$$c_9 = \{(1/2 + kR^2/8) \cdot I_1(kR) - (kR/4 + kR^3/32) \cdot I_0(kR),$$
$$(kR/4 + kR^3/32) \cdot I_0(kR) - (1/2 + kR^2/8) \cdot I_1(kR),$$
$$kR^2/16 \cdot I_1(kR) - (kR/4 + kR^3/48) \cdot I_2(kR),$$
$$kR^3/96 \cdot I_2(kR) - kR^2/16 \cdot I_3(kR),$$
$$-(1/2 + kR^2/8) \cdot K_1(kR) - (kR/4 + kR^3/32) \cdot K_0(kR),$$
$$-(kR/4 + kR^3/32) \cdot K_0(kR) - (1/2 + kR^2/8) \cdot K_1(kR),$$
$$-kR^2/16 \cdot K_1(kR) - (kR/4 + kR^3/48) \cdot K_2(kR),$$
$$-kR^3/96 \cdot K_2(kR) - kR^2/16 \cdot K_3(kR),$$
$$-1/kR, 0, 0, 0, 0, 0, 0\};$$

$$c_{10} = \{(kR/2 + kR^3/16) \cdot I_1(kR) - (1/2 + 3kR^2/16) \cdot I_0(kR),$$
$$(1/2 + 3kR^2/16) \cdot I_0(kR) - (1/(2kR) + 9kR/16 + 5kR^3/96) \cdot I_1(kR),$$
$$(kR/4 + kR^3/24) \cdot I_1(kR) - (3/4 + 5kR^2/24) \cdot I_2(kR),$$
$$kR^2/16 \cdot I_2(kR) - (5kR/16 + 5kR^3/192) \cdot I_3(kR),$$
$$-(kR/2 + kR^3/16) \cdot K_1(kR) - (1/2 + 3kR^2/16) \cdot K_0(kR),$$
$$-(1/2 + 3kR^2/16) \cdot K_0(kR) - (1/(2kR) + 9kR/16 + 5kR^3/96) \cdot K_1(kR),$$
$$-(kR/4 + kR^3/24) \cdot K_1(kR) - (3/4 + 5kR^2/24) \cdot K_2(kR),$$
$$-kR^2/16 \cdot K_2(kR) - (5kR/16 + 5kR^3/192) \cdot K_3(kR),$$
$$0, -1, 0, 0, 1/kR^2, 0, 0\};$$

$$c_{11} = \{kR^2/8 \cdot I_1(kR) - (kR/4 + kR^3/24) \cdot I_0(kR),$$
$$(kR/4 + kR^3/24) \cdot I_0(kR) - (1/2 + kR^2/6) \cdot I_1(kR),$$
$$(1/2 + kR^2/8) \cdot I_1(kR) - (1/kR + kR/2 + 7kR^3/192) \cdot I_2(kR),$$
$$(kR/4 + kR^3/32) \cdot I_2(kR) - (1 + 3kR^2/16) \cdot I_3(kR),$$
$$-kR^2/8 \cdot K_1(kR) - (kR/4 + kR^3/24) \cdot K_0(kR),$$
$$-(kR/4 + kR^3/24) \cdot K_0(kR) - (1/2 + kR^2/6) \cdot K_1(kR),$$
$$-(1/2 + kR^2/8) \cdot K_1(kR) - (1/kR + kR/2 + 7kR^3/192) \cdot K_2(kR),$$
$$-(kR/4 + kR^3/32) \cdot K_2(kR) - (1 + 3kR^2/16) \cdot K_3(kR),$$
$$0, 0, -2kR, 0, 0, 2/kR^3, 0\};$$

$c_{12} = \{kR^3/48 \cdot I_1(kR) - kR^2/16 \cdot I_0(kR),$

$\quad kR^2/16 \cdot I_0(kR) - (3kR/16 + 5kR^3/192) \cdot I_1(kR),$

$\quad (kR/4 + kR^3/32) \cdot I_1(kR) - (3/4 + 5kR^2/32) \cdot I_2(kR),$

$\quad (1/2 + kR^2/8) \cdot I_2(kR) - (3/(2kR) + 5kR/8 + kR^3/32) \cdot I_3(kR),$

$\quad -kR^3/48 \cdot K_1(kR) - kR^2/16 \cdot K_0(kR),$

$\quad -kR^2/16 \cdot K_0(kR) - (3kR/16 + 5kR^3/192) \cdot K_1(kR),$

$\quad -(kR/4 + kR^3/32) \cdot K_1(kR) - (3/4 + 5kR^2/32) \cdot K_2(kR),$

$\quad -(1/2 + kR^2/8) \cdot K_2(kR) - (3/(2kR) + 5kR/8 + kR^3/32) \cdot K_3(kR),$

$\quad 0, 0, 0, -3kR^2, 0, 0, 3/kR^4\};$

$c_{13} = \{kR/8 \cdot I_0(kR) + (1/2 + kR^2/16) \cdot I_1(kR),$

$\quad (-1/(2kR) + kR/16 + kR^3/96) \cdot I_0(kR) + (1/kR^2 + kR^2/48) \cdot I_1(kR),$

$\quad -(3/4 + kR^2/24) \cdot I_1(kR) + 3/(2kR) \cdot I_2(kR),$

$\quad -(5kR/16 + kR^3/192) \cdot I_2(kR) + 5/8 \cdot I_3(kR),$

$\quad kR/8 \cdot K_0(kR) - (1/2 + kR^2/16) \cdot K_1(kR),$

$\quad (1/(2kR) - kR/16 - kR^3/96) \cdot K_0(kR) + (1/kR^2 + kR^2/48) \cdot K_1(kR),$

$\quad (3/4 + kR^2/24) \cdot K_1(kR) + 3/(2kR) \cdot K_2(kR),$

$\quad (5kR/16 + kR^3/192) \cdot K_2(kR) + 5/8 \cdot K_3(kR),$

$\quad 0, 0, 0, 0, -2/kR^3, 0, 0\};$

$c_{14} = \{(1/4 + kR^2/16) \cdot I_0(kR) + (kR/4 + kR^3/48) \cdot I_1(kR),$

$\quad (kR^2 \cdot I_0(kR))/24 + (kR \cdot I_1(kR))/24,$

$\quad (-1/kR - kR/4 + kR^3/192) \cdot I_1(kR) + (1/4 + 3/kR^2 + kR^2/192) \cdot I_2(kR),$

$\quad (-1 - kR^2/8) \cdot I_2(kR) + (3/kR + kR/8) \cdot I_3(kR),$

$\quad (1/4 + kR^2/16) \cdot K_0(kR) + (-kR/4 - kR^3/48) \cdot K_1(kR),$

$\quad -(kR^2 \cdot K_0(kR))/24 + (kR \cdot K_1(kR))/24,$

$\quad (1/kR + kR/4 - kR^3/192) \cdot K_1(kR) + (1/4 + 3/kR^2 + kR^2/192) \cdot K_2(kR),$

$\quad (1 + kR^2/8) \cdot K_2(kR) + (3/kR + kR/8) \cdot K_3(kR),$

$\quad 0, 0, 2, 0, 0, -6/kR^4, 0\};$

$c_{15} = \{(kR \cdot I_0(kR))/8 + (kR^2 \cdot I_1(kR))/16,$

$\quad (kR/16 + kR^3/64) \cdot I_0(kR) + (kR^2 \cdot I_1(kR))/32,$

$\quad (-1/4 - kR^2/32) \cdot I_1(kR) + I_2(kR)/(2kR),$

$\quad (-3/(2kR) - (3kR)/8) \cdot I_2(kR) + (3/4 + 6/kR^2) \cdot I_3(kR),$

$\quad (kR \cdot K_0(kR))/8 - (kR^2 \cdot K_1(kR))/16,$

$\quad (-kR/16 - kR^3/64) \cdot K_0(kR) + (kR^2 \cdot K_1(kR))/32,$

$\quad (1/4 + kR^2/32) \cdot K_1(kR) + K_2(kR)/(2kR),$

$\quad (3/(2kR) + (3kR)/8) \cdot K_2(kR) + (3/4 + 6/kR^2) \cdot K_3(kR),$

$\quad 0, 0, 0, 6kR, 0, 0, -12/kR^5\}.$

Identities: $ka^{11} = (ka)^{11}$; $kR^n = (kR)^n$.

The diagram below shows the field of the magnitude $|\vec{V}/U|$ of the total velocity $\vec{V}$ to the incoming velocity U for $ka = 0.001$; $R/a = 10$.

$|V(r/a, \varphi)/U|$; $ka = 0.001$; $R/a = 10$
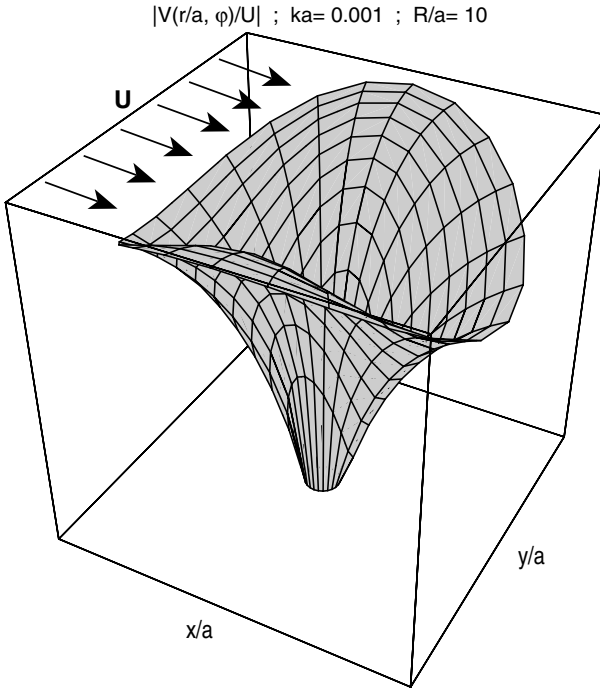
Field of total velocity magnitude around a fibre in a regular fibre array with transversal incoming flow U

On each fibre acts a pressure force F_{xp} and a viscous force F_{xv} in the x direction:

$$F_{xp} = -\int_0^{2\pi} a\, p\, d\varphi \quad ; \quad F_{xv} = -\int_0^{2\pi} a\eta \cdot \frac{\partial \vec{V}_\varphi}{\partial r}\bigg|_{r=a} \cdot \cos\vartheta d\varphi. \tag{7}$$

Their values are:

$$\frac{F_{xp}}{\frac{1}{2}\rho U^2 \cdot 2a} = \pi \cdot \left(\frac{C_0}{ka} + 2\,ka\,C_2 \right), \tag{8}$$

$$
\begin{aligned}
\frac{F_{xv}}{\frac{1}{2}\rho U^2 \cdot 2a} = -\pi \cdot \Bigg\{ & \left[ka \left(\frac{1}{16} + \frac{ka^2}{192} + \frac{ka^4}{6144} \right) I_0(ka) \right. \\
& + \left. \left(\frac{1}{4} + \frac{ka^2}{32} + \frac{ka^4}{768} + \frac{ka^6}{36864} \right) I_1(ka) \right] \cdot A_0 + \left[\left(-\frac{1}{4ka} + \frac{ka}{32} + \frac{ka^3}{256} + \frac{5\,ka^5}{36864} \right) I_0(ka) \right. \\
& + \left. \left(\frac{1}{2\,ka^2} + \frac{ka^2}{128} + \frac{5\,ka^4}{9216} \right) I_1(ka) \right] \cdot A_1 + \left[-\left(\frac{3}{8} + \frac{ka^2}{48} + \frac{ka^4}{3072} - \frac{ka^6}{92160} \right) I_1(ka) \right. \\
& + \left. \left(\frac{3}{4\,ka} - \frac{ka^3}{1536} + \frac{ka^5}{23040} \right) I_2(ka) \right] \cdot A_2 + \left[-\left(\frac{5\,ka}{32} + \frac{13\,ka^3}{1536} + \frac{11\,ka^5}{61440} \right) I_2(ka) \right. \\
& + \left. \left(\frac{5}{16} - \frac{11\,ka^4}{30720} \right) I_3(ka) \right] \cdot A_3 + \left[ka \left(\frac{1}{16} + \frac{ka^2}{192} + \frac{ka^4}{6144} \right) K_0(ka) \right. \\
& - \left. \left(\frac{1}{4} + \frac{ka^2}{32} + \frac{ka^4}{768} + \frac{ka^6}{36864} \right) K_1(ka) \right] \cdot B_0 + \left[\left(\frac{1}{4ka} - \frac{ka}{32} - \frac{ka^3}{256} - \frac{5\,ka^5}{36864} \right) K_0(ka) \right. \\
& + \left. \left(\frac{1}{2\,ka^2} + \frac{ka^2}{128} + \frac{5\,ka^4}{9216} \right) K_1(ka) \right] \cdot B_1 + \left[\left(\frac{3}{8} + \frac{ka^2}{48} + \frac{ka^4}{3072} - \frac{ka^6}{92160} \right) K_1(ka) \right. \\
& + \left. \left(\frac{3}{4\,ka} - \frac{ka^3}{1536} + \frac{ka^5}{23040} \right) K_2(ka) \right] \cdot B_2 + \left[\left(\frac{5\,ka}{32} + \frac{13\,ka^3}{1536} + \frac{11\,ka^5}{61440} \right) K_2(ka) \right. \\
& + \left. \left(\frac{5}{16} - \frac{11\,ka^4}{30720} \right) K_3(ka) \right] \cdot B_3 - \frac{1}{ka^3} \cdot D_1 \Bigg\}.
\end{aligned}
\tag{9}
$$

For small $ka \ll 1$ a power series development of the modified Bessel functions in F_{xv} gives the approximation:

$$
\begin{aligned}
\frac{F_{xv}}{\frac{1}{2}\rho U^2 \cdot 2a} = -\pi \cdot \Bigg\{ & [0.1875\,ka + 0.0520833\,ka^2] \cdot A_0 \\
& + [2.63111 \cdot 10^{-8}\,ka + 0.0130208\,ka^3] \cdot A_1 \\
& + [-0.093750\,ka - 0.0260416\,ka^3] \cdot A_2 \\
& + [1.31556 \cdot 10^{-7}\,ka - 0.013021\,ka^3] \cdot A_3 \\
& + [-0.25/ka - 0.076978\,ka + 0.0116033\,ka^3 - (0.1875\,ka \\
& \quad + 0.0520833\,ka^3)\,\ln ka] \cdot B_0 \\
& + [0.5/ka^3 - 0.125/ka + 0.0312499\,ka + 0.00198205\,ka^3 \\
& \quad + (2.63111 \cdot 10^{-8}\,ka + 0.0130208\,ka^3)\,\ln ka] \cdot B_1 \\
& + [1.5/ka^3 + 4.500 \cdot 10^{-8}/ka + 0.0502076\,ka - 0.00766781\,ka^3 \\
& \quad + (0.09375008\,ka + 0.0260416\,ka^3)\,\ln ka] \cdot B_2 \\
& + [2.5/ka^3 + 7.500 \cdot 10^{-8}/ka - 0.02500025\,ka - 0.00235060\,ka^3 \\
& \quad + (1.315556 \cdot 10^{-7}\,ka - 0.0130210\,ka^3)\,\ln ka] \cdot B_3 - \frac{1}{ka^3} \cdot D_1 \Bigg\}.
\end{aligned}
\tag{10}
$$

The test sample of a model material with regular fibre arrangement is supposed to have the dimensions D_x in the flow direction and D_y normal to the flow and to the fibres. The flow resistivity $\Xi_\perp$ is given by the sum of the viscous forces on the fibres in the sample:

$$\Xi_\perp = \frac{2\eta \cdot \sum\limits_{i=1}^{I} ka_i \dfrac{F_{xv,i}(ka_i, kR_i)}{a_i \rho_0 U^2}}{D_x D_y (1 - \mu)} \tag{11}$$

with η the dynamic viscosity, $\mu = 1 - \sigma$ the massivity of the material, and $D_x D_y = I \cdot \pi \langle R_i^2 \rangle$. The terms under the sum in the numerator are nearly independent of ka_i, so they are a function $c(R_i/a_i)$ of the remaining parameter R_i/a_i. This function can be evaluated by (a regression through the values from the cell model):

$$c\left(\frac{R}{a}\right) = e^{f(x)} \quad ; \quad x = \ln\frac{R}{a},$$

$$f(x) = 0.865823 + \frac{0.0250214}{x^3} - \frac{0.322560}{x^2} + \frac{1.78839}{x} \tag{12}$$

$$- 0.530524\, x + 0.0604543\, x^2 - 0.00312698\, x^3.$$
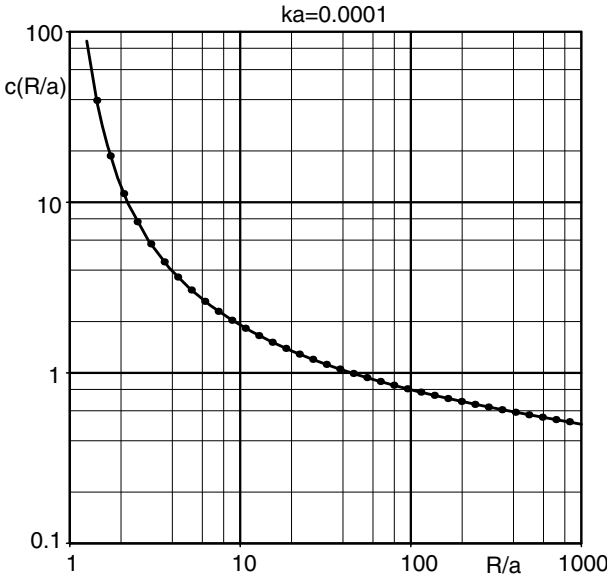
Function c(R/a) of the sum terms in the numerator of $\Xi_\perp$. Points: from the model theory; curve: regression. The curves coincide if ka is varied by powers of ten

If the fibre and cell radii are randomised with relative frequencies q_m of the fibre radius a_i in the counting group with mean value a_m, and correspondingly p_n the relative frequency of R_i in the counting group around R_n, the flow resistivity $\Xi_\perp$ is:
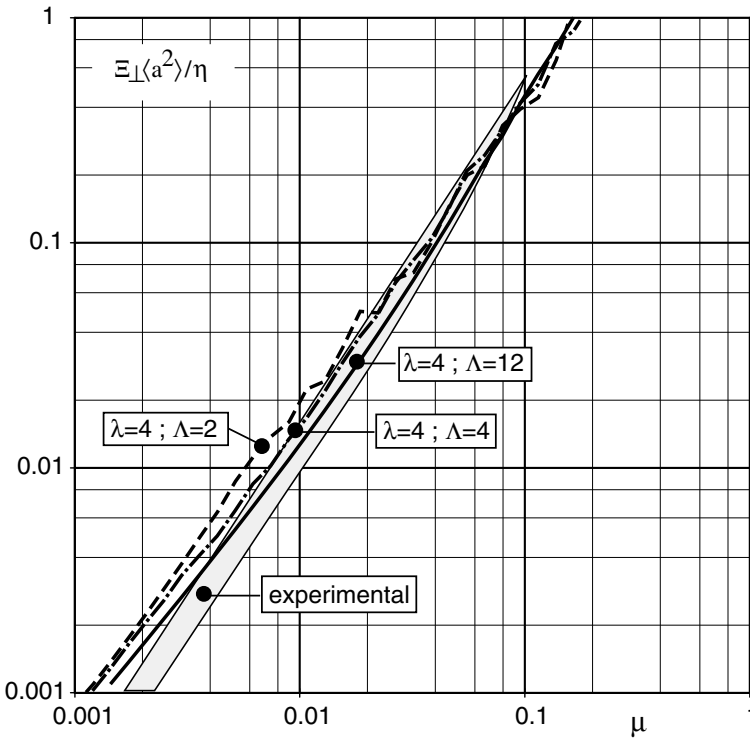
$$\Xi_\perp \frac{<a^2>}{\eta} = \frac{2\mu}{\pi(1 - \mu)} \cdot \sum_{m,n} q_m\, p_n \cdot c\left(\frac{R_n}{a_m}\right). \tag{13}$$

If the relative frequencies are Poisson distributions:

$$q_m = e^{-\lambda} \cdot \frac{\lambda^m}{m!} \quad ; \quad p_n = e^{-\Lambda} \cdot \frac{\Lambda^n}{n!} \quad ; \quad m, \ n = 0, \ 1, \ 2, \dots, \tag{14}$$

then the needed radius ratios are:

$$\frac{R_n}{a_m} = \frac{n + 1/2}{m + 1/2} \frac{1}{\sqrt{\mu}} \sqrt{\frac{\lambda^2 + 2\lambda + 1/4}{\Lambda^2 + 2\Lambda + 1/4}}. \tag{15}$$

Flow resistivity $\Xi_\perp$ of a bundle of parallel fibres for transversal flow. Computed curves with different parameters of the Poisson distributions, and shaded range of experimental data

G.8   Transversal Sound in Parallel Fibres

The model of the porous material is illustrated in ❯ *Sect. G.5*, but the sound propagation is transversal to the fibres, which are supposed to be at rest. An elementary cell and the used co-ordinates are shown here.

The direction of the incident wave is v_i. The sound field in a cell is evaluated with density and viscous and thermal waves taken into account.

The cell radius R is determined so that, with the given fibre radius a, the desired massivity µ is obtained.
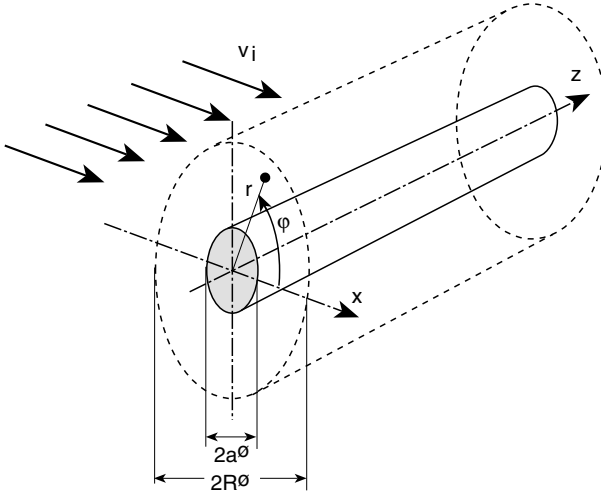
In a first model (*closed-cell model*) the cell surfaces are adiabatic surfaces of symmetry for the field scattered at a fibre (the scattered fields do not penetrate the cell surface, but the surface is transparent for the incident wave); in a second model the scattered field freely propagates through the fibre bundle (*open-cell model*); this model is ultimately used to evaluate multiple scattering between fibres (*multiple scattering model*). The advantage of the multiple scattering model is that it permits random fibre distances.

The characteristic propagation constant Γ_i and wave impedance Z_i of the density wave in the fibre bundle are determined from the effective density ρ_{eff} and effective compressibility C_{eff} by:

$$\frac{\Gamma_i}{k_0} = j\sqrt{\frac{\rho_{eff}}{\rho_0} \cdot \frac{C_{eff}}{C_0}} \quad ; \quad \frac{Z_i}{Z_0} = \sqrt{\frac{\rho_{eff}}{\rho_0} \Big/ \frac{C_{eff}}{C_0}}, \tag{1}$$

which in turn are evaluated by the integrals:

$$\frac{\rho_{eff}}{\rho_0} = \frac{\oint \left[\Phi_i + \Phi_\rho + \frac{\Pi_\alpha}{\Pi_\rho}\Phi_\alpha\right] \cdot \cos\varphi\, ds}{\oint [\Phi_i + \Phi_\rho + \Phi_\alpha] \cdot \cos\varphi\, ds - \int\limits_0^{2\pi} d\varphi \int\limits_a^R \left(\frac{\partial \Psi_z}{\partial\varphi}\cos\varphi + r\frac{\partial \Psi_z}{\partial r}\sin\varphi\right) dr}, \tag{2}$$

$$\frac{C_{eff}}{C_0} = \frac{R\int\limits_0^{2\pi} v_{ir}(R, \varphi)d\varphi}{k_\rho^2 \iint\limits_{A_0} \left[(\Phi_e + \Phi_\rho) + \frac{\Pi_\alpha}{\Pi_\rho}\Phi_\alpha\right] dA}. \tag{3}$$

Here Φ_i is the potential function of the incident density wave; Φ_ρ, Φ_α are the potentials of the scattered density and thermal waves; Ψ_z is the z component of the vector potential of the scattered viscous wave; k_ρ, k_α, k_ν are the free field wave numbers of the density, thermal and viscous waves, respectively; for the factors Π_ρ, Π_α see ❯ *Sects. J.1–J.3*. The integrals $\oint$ ... ds are taken over the surface of the cell; the integral over A_0 is over the cell area. The field components of the scattered field are formulated as Fourier series over φ; the index $\beta = \rho$, α stands for the density and thermal wave types:

Closed-cell model:

Fourier series formulations of the component fields:

$$\Phi_\beta(r, \varphi) = \sum_{n=0} [A_{\beta n} H_n^{(2)}(k_\beta r) + B_{\beta n} J_n(k_\beta r)] \cdot \cos(n\varphi)$$

$$= \sum_{n=0} \Phi_{\beta rn}(r) \cdot \cos(n\varphi) \quad ; \quad \beta = \rho, \ \alpha,$$

(4)

$$\vec{\Psi} = \{0, \ 0, \ \Psi_z\} \ ,$$

$$\Psi_z(r, \varphi) = \sum_{n=0} [A_{\nu n} H_n^{(2)}(k_\nu r) + B_{\nu n} J_n(k_\nu r)] \cdot \sin(n\varphi)$$

(5)

$$= \sum_{n=0} \Psi_{\nu rn}(r) \cdot \sin(n\varphi).$$

The boundary conditions at the cell and fibre surfaces are (for each Fourier series term):

$$k_\rho R \ \Phi'_{\rho rn}(R) + k_\alpha R \ \Phi'_{\alpha rn}(R) - n \ \Psi_{zrn}(R) = 0$$

$$-n \ [\Phi_{\rho rn}(R) + \Phi_{\alpha rn}(R)] + n \ [k_\rho R \ \Phi'_{\rho rn}(R) + k_\alpha R \ \Phi'_{\alpha rn}(R)] - (k_\nu R)^2 \Psi''_{zrn}(R) = 0$$

(6)

$$k_\rho R \ \Phi'_{\rho rn}(R) + \frac{\Theta_\alpha}{\Theta_\rho} k_\alpha R \ \Phi'_{\alpha rn}(R) = 0,$$

$$n \ [\Phi_{\rho rn}(a) + \Phi_{\alpha rn}(a)] - k_\nu a \ \Psi'_{zrn}(a) = -n \ \Phi_{ern}(a)$$

$$k_\rho R \ \Phi'_{\rho rn}(a) + k_\alpha R \ \Phi'_{\alpha rn}(a) - n \ \Psi_{zrn}(a) = -k_\rho a \ \Phi'_{ern}(a)$$

(7)

$$\Phi_{\rho rn}(a) + \frac{\Theta_\alpha}{\Theta_\rho} \Phi_{\alpha rn}(a) = -\Phi_{ern}(a),$$

(for the factors Θ_ρ, Θ_α see ❯ *Sects. J.1–J.3*; the prime indicates the derivative with respect to the argument of the radial functions in the field terms). The inhomogeneous linear systems of equations can be solved for the amplitudes of the Fourier terms (see Mechel (1995), Ch. 12) for more details). The integrals for ρ_{eff} and C_{eff} need only the terms n = 0 for the effective compressibility and n = 1 for the effective density (other

integrals vanish); so the final equations are (A_i is the arbitrary amplitude of the incident density wave) as follows:

$$\frac{\rho_{eff}}{\rho_0} = \frac{(-2jA_i + B_{\rho 1})[J_1(k_\rho R) - \frac{a}{R}J_1(k_\rho a)] + A_{\rho 1}[H_1^{(2)}(k_\rho R) - \frac{a}{R}H_1^{(2)}(k_\rho a)] + \ldots}{(-2jA_i + B_{\rho 1})[J_1(k_\rho R) - \frac{a}{R}J_1(k_\rho a)] + A_{\rho 1}[H_1^{(2)}(k_\rho R) - \frac{a}{R}H_1^{(2)}(k_\rho a)] + \ldots}$$

$$\frac{\ldots + \frac{\Pi_\alpha}{\Pi_\rho}\left[A_{\alpha 1}[H_1^{(2)}(k_\alpha R) - \frac{a}{R}H_1^{(2)}(k_\alpha a)] + B_{\alpha 1}[J_1(k_\alpha R) - \frac{a}{R}J_1(k_\alpha a)]\right]}{\ldots + A_{\alpha 1}[H_1^{(2)}(k_\alpha R) - \frac{a}{R}H_1^{(2)}(k_\alpha a)] + B_{\alpha 1}[J_1(k_\alpha R) - \frac{a}{R}J_1(k_\alpha a)] - \ldots}$$

$$\frac{\cdots}{-A_{\nu 1}[H_1^{(2)}(k_\nu R) - \frac{a}{R}H_1^{(2)}(k_\nu a)] - B_{\nu 1}[J_1(k_\nu R) - \frac{a}{R}J_1(k_\nu a)]} , \tag{8}$$

$$\frac{C_{eff}}{C_0} = \frac{k_\rho R \, J_1(k_\rho R) \, A_i}{(A_i + B_{\rho 0})[yJ_1(y)]_{k_\rho a}^{k_\rho R} + A_{\rho 0}[yH_1^{(2)}(y)]_{k_\rho a}^{k_\rho R} + \ldots}$$

$$\frac{\cdots}{\ldots + \frac{\Pi_\alpha}{\Pi_\rho}\frac{k_\rho^2}{k_\alpha^2}\left[A_{\alpha 0}[yH_1^{(2)}(y)]_{k_\alpha a}^{k_\alpha R} + B_{\alpha 0}[yJ_1(y)]_{k_\alpha a}^{k_\alpha R}\right]} . \tag{9}$$

with $[f(y)]_a^b = f(b) - f(a)$.

The free field wave numbers k_ρ, k_α, k_ν can be reduced to $k_0 = \omega/c_0$ (c_0 = adiabatic sound velocity) and $k_\nu^2 = -j\,\omega/\nu$ (ν = kinematic viscosity; see section "Sound in capillaries"), and k_ν in turn can be related to the flow resistivity Ξ of a transversal fibre bundle with the absorber variable $E = \rho_0 f/\Xi$ by the relation

$$|k_\nu a|^2 = \frac{4\mu}{1 - \mu} \cdot c\left(\frac{R}{a}\right) \cdot E \tag{10}$$

with the massivity μ and the function $c(R/a)$ from ▶ *Sect. G.7*.

The real part of the characteristic impedance from the transversal fibre closed-cell model typically shows a resonance because of the assumedly identical interactions of the fibres with the cell surfaces in all cells (the closed cell model cannot handle the time lag of scattering during the propagation through the bundle).

Open-cell model:

The potentials of the incident density wave Φ_i and of the scattered waves Φ_β; $\beta = \alpha, \nu$ (scattered density and temperature wave) as well as the scattered viscosity wave Ψ are formulated as:

$$\Phi_i(r, \varphi) = A_i \cdot e^{-jk_\rho x} = A_i \sum_{n \geq 0} \delta_n(-j)^n \cdot J_n(k_\rho r) \cdot \cos(n\varphi)$$

$$= \sum_{n \geq 0} \Phi_{irn}(r) \cdot \cos(n\varphi) \quad ; \quad \delta_n = \begin{cases} 1; & n = 0 \\ 2; & n > 0 \end{cases} , \tag{11}$$
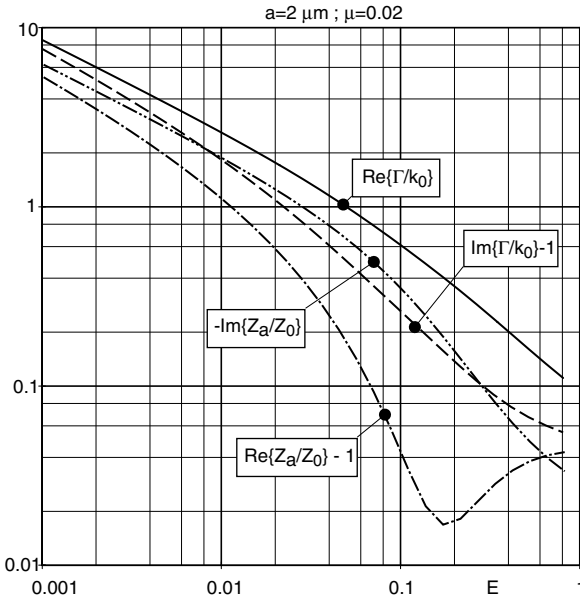
Characteristic values of a transversal fibre bundle evaluated with the closed-cell model of regular arrangement

$$\Phi_\beta(r, \varphi) = \sum_{n \geq 0} A_{\beta n} H_n^{(2)}(k_\beta r) \cdot \cos(n\varphi)$$
$$= \sum_{n \geq 0} \Phi_{\beta r n}(r) \cdot \cos(n\varphi) \quad ; \quad \beta = \rho, \; \alpha, \tag{12}$$

$$\vec{\Psi} = \{0, \; 0, \; \Psi_z\},$$

$$\Psi_z(r, \varphi) = \sum_{n \geq 0} A_{\nu n} H_n^{(2)}(k_\nu r) \cdot \sin(n\varphi) \tag{13}$$
$$= \sum_{n \geq 0} \Psi_{\nu r n}(r) \cdot \sin(n\varphi).$$

The scattered field amplitudes follow from the system of linear equations ($n = 0, 1$) which represent the boundary conditions:

$$\sum_{\beta = \rho, \alpha} A_{\beta n} n \, H_n^{(2)}(k_\beta a) - A_{\nu n} \, [k_\nu a \, H_{n-1}^{(2)}(k_\nu a) - n \, H_n^{(2)}(k_\nu a)]$$

$$= -n \, \delta_n \, (-j)^n J_n(k_\rho a) \, A_i$$

$$\sum_{\beta = \rho, \alpha} A_{\beta n} [k_\beta a \, H_{n-1}^{(2)}(k_\beta a) - n \, H_n^{(2)}(k_\beta a)] - A_{\nu n} \, n \, H_n^{(2)}(k_\nu a) \tag{14}$$

$$= - \, \delta_n \, (-j)^n [k_\rho a \, J_{n-1}(k_\rho a) - n \, J_n(k_\rho a)] \, A_i$$

$$A_{\rho n} H_n^{(2)}(k_\rho a) + \frac{\Theta_\alpha}{\Theta_\rho} A_{\alpha n} H_n^{(2)}(k_\alpha a) = - \, \delta_n \, (-j)^n J_n(k_\rho a) \, A_i,$$

and with them the effective density ρ_{eff} and effective compressibility C_{eff} are evaluated from:

$$\frac{\rho_{eff}}{\rho_0} = \frac{-2jA_i[J_1(k_\rho R) - \frac{a}{R}J_1(k_\rho a)] + A_{\rho 1}[H_1^{(2)}(k_\rho R) - \frac{a}{R}H_1^{(2)}(k_\rho a)] + \dots}{-2jA_i[J_1(k_\rho R) - \frac{a}{R}J_1(k_\rho a)] + A_{\rho 1}[H_1^{(2)}(k_\rho R) - \frac{a}{R}H_1^{(2)}(k_\rho a)] + \dots}$$

$$\frac{\dots + \frac{\Pi_\alpha}{\Pi_\rho}A_{\alpha 1}[H_1^{(2)}(k_\alpha R) - \frac{a}{R}H_1^{(2)}(k_\alpha a)]}{\dots + A_{\alpha 1}[H_1^{(2)}(k_\alpha R) - \frac{a}{R}H_1^{(2)}(k_\alpha a)] - A_{\nu 1}[H_1^{(2)}(k_\nu R) - \frac{a}{R}H_1^{(2)}(k_\nu a)]},$$

(15)

$$\frac{C_{eff}}{C_0} = \frac{A_i \, k_\rho R \, J_1(k_\rho R) + A_{\rho 0} \, k_\rho R \, H_1^{(2)}(k_\rho R) + A_{\alpha 0} \, k_\alpha R \, H_1^{(2)}(k_\alpha R)}{A_i \, [yJ_1(y)]_{k_\rho a}^{k_\rho R} + A_{\rho 0} \, [yH_1^{(2)}(y)]_{k_\rho a}^{k_\rho R} + \frac{\Pi_\alpha}{\Pi_\rho} \frac{k_\rho^2}{k_\alpha^2} A_{\alpha 0} \, [yH_1^{(2)}(y)]_{k_\alpha a}^{k_\alpha R}}$$

(16)

with $[f(y)]_a^b = f(b) - f(a)$.

The characteristic values Γ and Z_i of the propagation constant and wave impedance of the sound wave propagating through the open-cell model fibre bundle approach realistic values only at relatively high values of $|k_\nu a|^2 = \omega a^2/\nu$; at low values the presence of the fibres is under-weighted. This is the consequence of the assumedly missing scatter interaction between neighbour fibres at low frequencies, where the viscous boundary layer at the fibres fills the whole interspace between the fibres in reality. Nevertheless, the open-cell model is needed for the evaluation of the scattered field in the multiple scattering model.
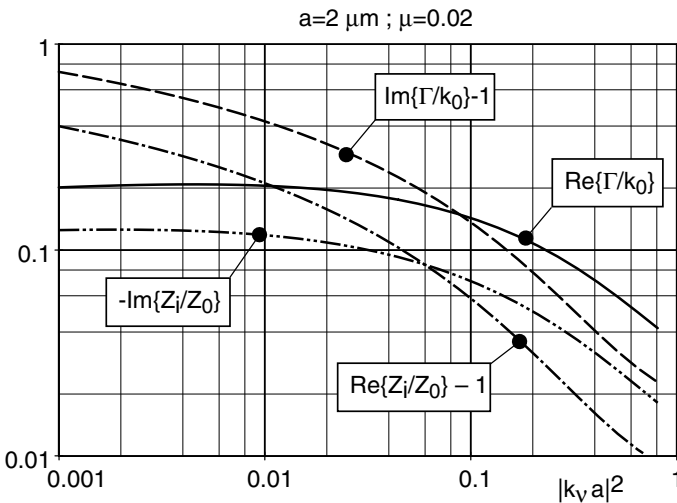
Characteristic values in a transversal fibre bundle evaluated with the open-cell model, which contains only single scattering at a fibre

Multiple scattering model:

This model considers the scattering at a reference fibre (in position P_i) at which not only the incident wave p_i is scattered but also the scattered fields coming from neighbour fibres (in positions P_j).
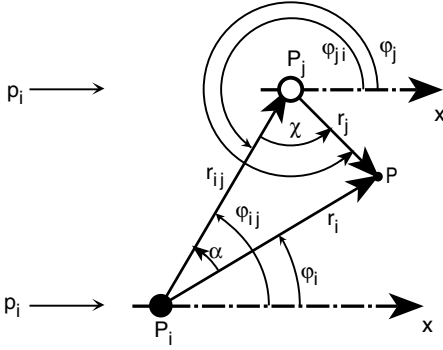
A minimum distance d between the reference fibre and the neighbour fibres is assumed. The fibres outside the range d may be arranged randomly with a porosity σ or massivity μ or fibre number density N of the transversal fibre bundle:

$$\sigma = 1 - \mu = 1 - N \cdot \pi a^2. \tag{17}$$

The "radiating" scattered fields, i.e. the scattered fields which assumedly propagate freely through the bundle, are indicated with a prime (with r, φ the co-ordinates centred in the scattering fibre):

$$\Phi'_{\beta}(r, \varphi) = \sum_{n=0}^{\infty} A_{\beta n} \cdot H_n^{(2)}(k_{\beta} r) \cdot \cos n\varphi \quad ; \quad \beta = \rho, \ \alpha$$

$$\Psi'_z(r, \varphi) = \sum_{n=0}^{\infty} A_{vn} \cdot H_n^{(2)}(k_v r) \cdot \sin n\varphi \quad ; \quad A_{v0} = 0. \tag{18}$$

The total scattered field in a point of immission P is indicated with a double prime; it is obtained by integration over the contributions of all neighbour fibres to the reference fibre. If the point of immission P is in position P_i of the reference fibre, the total scattered field is:

$$\Phi''_{\beta}(r_i, \varphi_i) = \int_0^{2\pi} d\varphi_{ij} \int_a^{\infty} N(r_{ij}) \cdot \Phi'_{\beta}(r_j, \varphi_j) \ r_{ij} dr_{ij}$$

$$= N \sum_{n \geq 0} A_{\beta n} \cdot \int_0^{2\pi} \int_d^{\infty} H_n^{(2)}(k_{\beta} r_j) \ r_{ij} \cos n\varphi_j dr_{ij} d\varphi_{ij}, \tag{19}$$

$$\Psi''_z(r_i, \varphi_i) = \int_0^{2\pi} d\varphi_{ij} \int_a^{\infty} N(r_{ij}) \cdot \Psi'_z(r_j, \varphi_j) \ r_{ij} dr_{ij}$$

$$= N \sum_{n \geq 0} A_{vn} \cdot \int_0^{2\pi} \int_d^{\infty} H_n^{(2)}(k_v r_j) \ r_{ij} \cdot \sin n\varphi_j dr_{ij} d\varphi_{ij}. \tag{20}$$

(the first expressions also permit a variable fibre density function $N(r_{ij})$). After application of the addition theorem for Hankel functions, to transform all co-ordinates to those of the reference fibre, one gets for the total scattered field around the reference fibre:

$$\Phi_\beta(r_i,\ \varphi_i) = \sum_{n \geq 0} A_{\beta n} \cdot [H_n^{(2)}(k_\beta r_i) \cdot \cos(n\varphi_i)$$

$$+ (-1)^n\ N \sum_{m=-\infty}^{\infty} \int_0^{2\pi} d\varphi_{ij} \int_d^{\infty} r_{ij} \cdot H_{n+m}^{(2)}(k_\beta r_{ij})$$

$$\cdot J_m(k_\beta r_i) \cdot \cos((n+m)\varphi_{ij} - m\,\varphi_i)dr_{ij}],$$

(21)

$$\Psi_z(r_i,\ \varphi_i) = \sum_{n \geq 0} A_{vn} \cdot [H_n^{(2)}(k_v r_i) \cdot \sin(n\varphi_i)$$

$$+ (-1)^n\ N \sum_{m=-\infty}^{\infty} \int_0^{2\pi} d\varphi_{ij} \int_d^{\infty} r_{ij} \cdot H_{n+m}^{(2)}(k_v r_{ij}) \cdot J_m(k_v r_i)$$

$$\cdot \sin((n+m)\varphi_{ij} - m\,\varphi_i)dr_{ij}]$$

with the geometrical relations

$$\varphi_{ji} = \varphi_{ij} + \pi$$

$$r_j\ = \sqrt{r_i^2 + r_{ij}^2 - 2\,r_i\,r_{ij}\ \cos(\varphi_{ij} - \varphi_i)}$$

(22)

$$\varphi_j\ = \varphi_{ji} + \text{arctg}\ \frac{r_i\ \sin(\varphi_{ij} - \varphi_i)}{r_{ij} - r_i\ \cos(\varphi_{ij} - \varphi_i)}.$$

In the above expressions for Φ_β, Ψ_z all integrals over φ_{ij} disappear except those with $m + n = 0$; then the integral returns the value 2π. Thus the total scattered field at the reference fibre becomes:

$$\Phi_\beta(r_i,\ \varphi_i) = \sum_{n \geq 0} A_{\beta n} \cdot \cos\ n\varphi_i \cdot [H_n^{(2)}(k_\beta r_i)$$
$$- \frac{2\pi N}{k_\beta^2} k_\beta d\ H_1^{(2)}(k_\beta d) \cdot J_n(k_\beta r_i)],$$

(23)

$$\Psi_z(r_i,\ \varphi_i) = \sum_{n \geq 0} A_{vn} \cdot \sin\ n\varphi_i \cdot [H_n^{(2)}(k_v r_i)$$
$$- \frac{2\pi N}{k_v^2} k_v d\ H_1^{(2)}(k_v d) \cdot J_n(k_v r_i)].$$

(24)

With these expressions plus the incident wave the boundary conditions at the reference fibre are satisfied. Using the abbreviations:

$$S_n(k_\beta y) = H_n^{(2)}(k_\beta y) - 2\ \frac{H_1^{(2)}(k_\beta R)}{k_\beta R} \cdot J_n(k_\beta y),$$

$$\beta = \rho,\ \alpha,\ v\ \ ;\ \ y = a,\ R,$$

(25)

$$A'_{\beta n} = \frac{A_{\beta n}}{A_i},$$

the needed scattered field amplitudes (normalised with the amplitude A_i of the incident density wave) are:

$$A'_{\rho 0} = -\frac{-k_\rho a\, J_1(k_\rho a)\, S_0(k_\alpha a) + \dfrac{\Theta_\rho}{\Theta_\alpha}\, k_\alpha a\, J_0(k_\rho a)\, S_1(k_\alpha a)}{-k_\rho a\, S_1(k_\rho a)\, S_0(k_\alpha a) + \dfrac{\Theta_\rho}{\Theta_\alpha}\, k_\alpha a\, S_0(k_\rho a)\, S_1(k_\alpha a)},$$

$$A'_{\alpha 0} = -\frac{\Theta_\rho}{\Theta_\alpha}\, \frac{-k_\rho a\, J_1(k_\rho a)\, S_0(k_\rho a) + k_\rho a\, J_0(k_\rho a)\, S_1(k_\rho a)}{-k_\rho a\, S_1(k_\rho a)\, S_0(k_\alpha a) - \dfrac{\Theta_\rho}{\Theta_\alpha}\, k_\alpha a\, S_0(k_\rho a)\, S_1(k_\alpha a)},$$

$$A'_{\rho 1} = -2j\, \frac{k_\nu a\, J_1(k_\rho a)\, S_0(k_\nu a) - k_\rho a\, k_\nu a\, J_0(k_\rho a)\, S_0(k_\nu a) + k_\rho a\, J_0(k_\rho a)\, S_1(k_\nu a)}{k_\rho a\, k_\nu a\, S_0(k_\rho a)\, S_0(k_\nu a) - \; k_\rho a\, S_0(k_\rho a)\, S_1(k_\nu a) - k_\nu a\, S_1(k_\rho a)\, S_0(k_\nu a)},$$

$$A'_{\nu 1} = -2j\, \frac{k_\rho a\, J_1(k_\rho a)\, S_0(k_\rho a) - k_\rho a\, J_0(k_\rho a)\, S_1(k_\rho a)}{k_\rho a\, k_\nu a\, S_0(k_\rho a)\, S_0(k_\nu a) - \; k_\rho a\, S_0(k_\rho a)\, S_1(k_\nu a) - k_\nu a\, S_1(k_\rho a)\, S_0(k_\nu a)}.$$

(26)

With these the effective density ρ_{eff} and compressibility C_{eff} are evaluated from:

$$\frac{\rho_{eff}}{\rho_0} = \left[1 - \frac{A'_{\nu 1} \cdot \left[S_1(k_\nu R) - \dfrac{a}{R}\, S_1(k_\nu a) \right]}{-2j\, \left[J_1(k_\rho R) - \dfrac{a}{R}\, J_1(k_\rho a) \right] + A'_{\rho 1} \cdot \left[S_1(k_\rho R) - \dfrac{a}{R}\, S_1(k_\rho a) \right]} \right]^{-1}, \qquad (27)$$

$$\frac{C_{eff}}{C_0} = \Bigg[1 - \frac{k_\rho a\, J_1(k_\rho a) + A'_{\rho 0} \cdot k_\rho a\, S_1(k_\rho a) + \ldots}{k_\rho R\, J_1(k_\rho R) + A'_{\rho 0} \cdot S_1(k_\rho R) + A'_{\alpha 0} \cdot k_\alpha R\, S_1(k_\alpha R)}$$
$$\frac{\ldots + A'_{\alpha 0} \cdot \left(\dfrac{\Pi_\alpha}{\Pi_\rho}\, \dfrac{k_\rho^2}{k_\alpha^2}\, (k_\alpha a\, S_1(k_\alpha a) - k_\alpha R\, S_1(k_\alpha R)) + k_\alpha R\, S_1(k_\alpha R) \right)}{\ldots} \Bigg]^{-1}.$$

(28)

Because mostly $k_\rho a \ll 1$, the following approximations are possible:

$$\frac{J_1(k_\rho a)}{k_\rho a \cdot J_0(k_\rho a)} \approx 1 \qquad ; \qquad \frac{J_1(k_\rho R)}{J_1(k_\rho a)} \approx \frac{1}{\sqrt{\mu}}$$

$$\frac{S_1(k_\rho R)}{S_1(k_\rho a)} \approx \frac{2 - \mu}{4\, \mu^{3/2}\, (1 - \mu)}\, (k_\rho a)^2 \ll 1 \qquad ; \qquad \frac{S_1(k_\rho a)}{k_\rho a \cdot S_0(k_\rho a)} \approx -\frac{1 - \mu}{2\mu}$$

$$\frac{\Theta_\rho \cdot k_\alpha^2}{\Theta_\alpha \cdot k_\rho^2} \approx -(\kappa - 1) \qquad ; \qquad \frac{\Pi_\alpha \cdot k_\rho^2}{\Pi_\rho \cdot k_\alpha^2} \ll 1.$$

(29)

If one introduces the abbreviation:

$$K_{1,0}(k_\beta a,\ \mu) = -\frac{2\mu}{1 - \mu} \cdot \frac{S_1(k_\beta a)}{k_\beta a\, S_0(k_\beta a)} \cdot \left(1 - \frac{1}{\sqrt{\mu}}\, \frac{S_1(k_\beta R)}{S_1(k_\beta a)} \right)$$
$$= -\frac{2\sqrt{\mu}}{1 - \mu} \cdot \frac{\sqrt{\mu}\, S_1(k_\beta a) - S_1(k_\beta R)}{k_\beta a \cdot S_0(k_\beta a)},$$

(30)

then the effective material data finally become with good precision:

$$\frac{\rho_{eff}}{\rho_0} \approx \frac{1}{1 - K_{1,0}(k_v a, \ \mu)} \quad ; \quad \frac{C_{eff}}{C_0} \approx 1 + (\kappa - 1) \cdot K_{1,0}(k_\alpha a, \ \mu) \tag{31}$$

(with κ = adiabatic exponent), and from these the characteristic values as usual are:

$$\frac{\Gamma_i}{k_0} = j\sqrt{\frac{\rho_{eff}}{\rho_0} \cdot \frac{C_{eff}}{C_0}} \quad ; \quad \frac{Z_i}{Z_0} = \sqrt{\frac{\rho_{eff}}{\rho_0} \Big/ \frac{C_{eff}}{C_0}}. \tag{32}$$

The following diagram shows the components of the characteristic data over $|k_v a|^2 = \omega a^2/\nu$ evaluated with these expressions. Numerical tests show that the ratio d/R of the minimum distance d of neighbour fibres to the reference fibre and the radius R of a cell around that fibre is important; the (reasonable) value $d/R = 1$ is recommended.
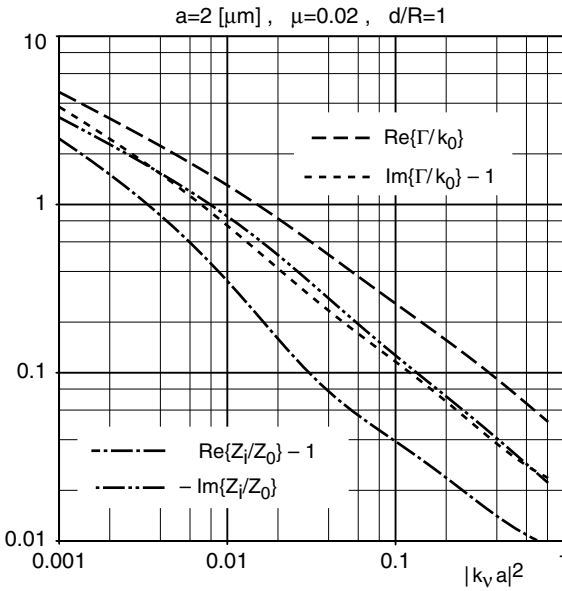
Components of the characteristic values of a transversal fibre bundle, evaluated with multiple scattering

The connection of the independent variable $|k_v a|^2$ with the flow resistivity variable $E = \rho_0 f/\Xi$ is required. This is given by ($\blacktriangleright$ Sect. G.7):

$$|k_v a|^2 = \frac{4\mu}{1 - \mu} \cdot c(x) \cdot E,$$

$$c\left(\frac{R}{a}\right) = e^{f(x)} \quad ; \quad x = \ln\frac{R}{a} = -0.5 \ \ln(\mu),$$

$$f(x) = 0.865823 + \frac{0.0250214}{x^3} - \frac{0.322560}{x^2} + \frac{1.78839}{x} - 0.530524 \ x$$

$$+ \ 0.0604543x^2 - 0.00312698x^3. \tag{33}$$

The multiple scattering model of a transversal fibre bundle only contains the function $K_{1,0}(k_\beta a, \mu)$ in the characteristic values. This function can be approximately represented by:

$$\text{Re}\{K_{1,0}(x, y)\} = 0, 51 - 0, 49 \cdot \tanh(2, 9 \cdot d_r(x, y)),$$

$$\text{Im}\{K_{1,0}(x, y)\} = \frac{h(x, y)}{\cosh^{3/2}(2, 5 \cdot d_i(x, y))},$$

$$d_r(x, y) = -0.5903666 - 0.8220386 \cdot x + 0.5694317 \cdot y, \tag{34}$$

$$d_i(x, y) = -0.494366 - 0.802776 \cdot x + 0.59628 \cdot y,$$

$$h(x, y) = -0.4959784 - 0.1499322/x + 0.003230626 \cdot x.$$

With these relations and $\quad (k_\nu a)^2 = -j \, |k_\nu a|^2 \quad ; \quad (k_\alpha a)^2 \approx \kappa \, \text{Pr} \cdot (k_\nu a)^2 \tag{35}$

(Pr = Prandtl number), the characteristic values of a transversal fibre bundle (with multiple scattering) can easily be evaluated. See the comparison below between exact evaluation and approximation.
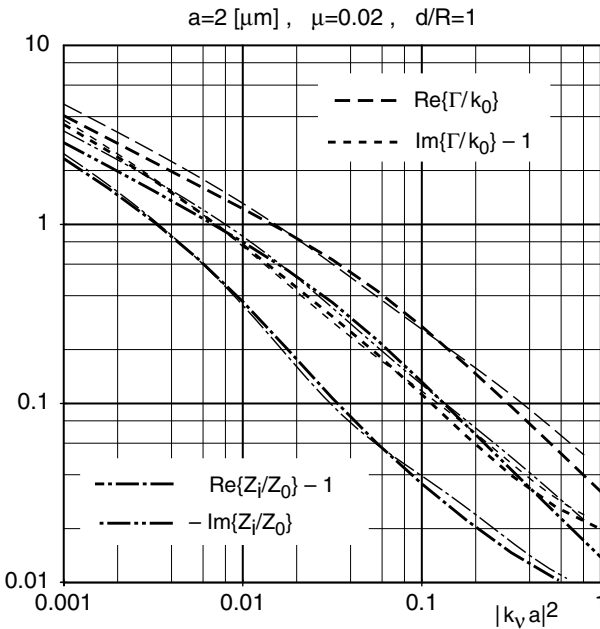
Comparison of the components of the characteristic values in a transversal fibre bundle from exact evaluation (thick lines) and approximation (thin lines)

G.9 Effective Wave Multiple Scattering in Transversal Fibre Bundle

As in ➤ *Sect. G.8* (with which this section has a number of similarities), the porous material consists of parallel fibres (at rest) with fibre radius a and fibre number density N. A sound wave propagates inside the fibre bundle normal to the fibres. Whereas it was assumed in ➤ *Sect. G.8* that the propagating wave is a density wave, here it is assumed to be a less specified "effective" wave with potential Φ_E having propagation constant $\Gamma = jk_e$. The propagating wave (exciting wave) may be some hybrid wave of a density wave, a thermal wave or a viscous wave. The propagation constant and wave impedance Z_e of this wave shall be determined. See ➤ *Sect. G.8* for the assumed co-ordinates. As before, the index $\beta = \rho$, α indicates a density or thermal wave with scalar potential functions Φ_β, and Ψ_z is the z component of the vector potential of a viscous wave. It is further assumed as before that the nearest neighbours of a reference fibre in the position (r_i, φ_i) are at a distance d from it.

Exciting wave formulation:

$$\Phi_E(r, \varphi) = A_E \cdot e^{-\Gamma x} = A_E \cdot e^{-jk_e r \cos\varphi} = A_E \cdot \sum_{n \geq 0} (-j)^n \, \delta_n \, J_n(k_e r) \, \cos(n\varphi)$$

$$= A_E \cdot \sum_{n \geq 0} \Phi_{Ern}(r) \cdot \cos(n\varphi) \quad ; \quad \delta_n = \begin{cases} 1 \; ; \; n = 0 \\ 2 \; ; \; n > 0. \end{cases} \tag{1}$$

Scattered field formulation (marked with a prime):

$$\Phi'_\beta(r, \varphi) = \sum_{n \geq 0} A_{\beta n} \, H_n^{(2)}(k_\beta r) \, \cos(n\varphi) = \sum_{n \geq 0} \Phi'_{\beta n}(r) \cdot \cos(n\varphi) \quad ; \quad \beta = \rho, \, \alpha,$$

$$\Psi'_z(r, \varphi) = \sum_{n \geq 0} A_{vn} \, H_n^{(2)}(k_v r) \, \sin(n\varphi) = \sum_{n \geq 0} \Psi'_{vn}(r) \cdot \sin(n\varphi) \quad ; \quad A_{v0} = 0. \tag{2}$$

Total scattered field at a reference fibre in (r_i, φ_i) (marked with a double prime):

$$\Phi''_\beta(r_i, \varphi_i) = N \sum_{n \geq 0} A_{\beta n} \int_0^{2\pi} d\varphi_{ij} \int_d^\infty e^{-jk_e r_{ij} \cos\varphi_{ij}} \cdot H_n^{(2)}(k_\beta r_j) \, \cos(n\varphi_j) \cdot r_{ij} dr_{ij},$$

$$\Psi''_z(r_i, \varphi_i) = N \sum_{n \geq 0} A_{vn} \int_0^{2\pi} d\varphi_{ij} \int_d^\infty e^{-jk_e r_{ij} \cos\varphi_{ij}} \cdot H_n^{(2)}(k_v r_j) \, \sin(n\varphi_j) \cdot r_{ij} dr_{ij}, \tag{3}$$

and after application of the addition theorem for Hankel functions and integration:

$$\Phi_\beta(r_i, \varphi_i) = \sum_{n \geq 0} \cos(n\varphi_i) \cdot \{A_{\beta n} \, H_n^{(2)}(k_\beta r_i)$$

$$- \frac{2\pi N}{k_\beta^2 - k_e^2} (-j)^n \, J_n(k_\beta r_i) \cdot \sum_{m \geq 0} j^m \, B_{\beta mn} \cdot A_{\beta m}\} \tag{4}$$

$$= \sum_{n \geq 0} \Phi_{\beta rn}(r_i) \cdot \cos(n\varphi_i),$$

$$\Psi_z(r_i, \varphi_i) = \sum_{n \geq 0} \sin(n\varphi_i) \cdot \{A_{\nu n} \, H_n^{(2)}(k_\nu r_i)$$

$$+ \frac{2\pi N}{k_\nu^2 - k_e^2} \, (-j)^n \, J_n(k_\nu r_i) \cdot \sum_{m \geq 0} j^m \, B_{\nu mn} \cdot A_{\nu m}\} \tag{5}$$

$$= \sum_{n \geq 0} \Psi_{zrn}(r_i) \cdot \sin(n\varphi_i)$$

with the following abbreviations for both $\beta = \rho, \alpha$:

$$B_{\beta mn} = k_e d \cdot [H_{m+n}^{(2)}(k_\beta d) \, J_{m+n-1}(k_e d) + H_{m-n}^{(2)}(k_\beta d) \, J_{m-n-1}(k_e d)]$$

$$- k_\beta d \cdot [H_{m+n-1}^{(2)}(k_\beta d) \, J_{m+n}(k_e d) + H_{m-n-1}^{(2)}(k_\beta d) \, J_{m-n}(k_e d)], \tag{6}$$

$$B_{\nu mn} = k_e d \cdot [H_{m+n}^{(2)}(k_\nu d) \, J_{m+n-1}(k_e d) - H_{m-n}^{(2)}(k_\nu d) \, J_{m-n-1}(k_e d)]$$

$$- k_\nu d \cdot [H_{m+n-1}^{(2)}(k_\nu d) \, J_{m+n}(k_e d) - H_{m-n-1}^{(2)}(k_\nu d) \, J_{m-n}(k_e d)].$$

These scattered waves plus the exciting wave have to satisfy the boundary conditions at the reference fibre (which is supposed to be isothermal):

$$v_\varphi(a, \varphi_i) = 0: \begin{cases} n \cdot [A_{\rho n} H_n^{(2)}(k_\rho a) - \dfrac{2\pi N}{k_\rho^2 - k_e^2} \, (-j)^n \, J_n(k_\rho a) \cdot \displaystyle\sum_{m \geq 0} j^m \, B_{\rho mn} \cdot A_{\rho m}] \\[2ex] + n \cdot [A_{\alpha n} H_n^{(2)}(k_\alpha a) - \dfrac{2\pi N}{k_\alpha^2 - k_e^2} \, (-j)^n \, J_n(k_\alpha a) \cdot \displaystyle\sum_{m \geq 0} j^m \, B_{\alpha mn} \cdot A_{\alpha m}] \\[2ex] - k_\nu a \cdot [A_{\nu n} H_n'^{(2)}(k_\nu a) + \dfrac{2\pi N}{k_\nu^2 - k_e^2} \, (-j)^n \, J_n'(k_\nu a) \cdot \displaystyle\sum_{m \geq 0} j^m \, B_{\nu mn} \cdot A_{\nu m}] \\[2ex] = -n \, \delta_n \, (-j)^n \, J_n(k_e a) \cdot A_E, \end{cases} \tag{7}$$
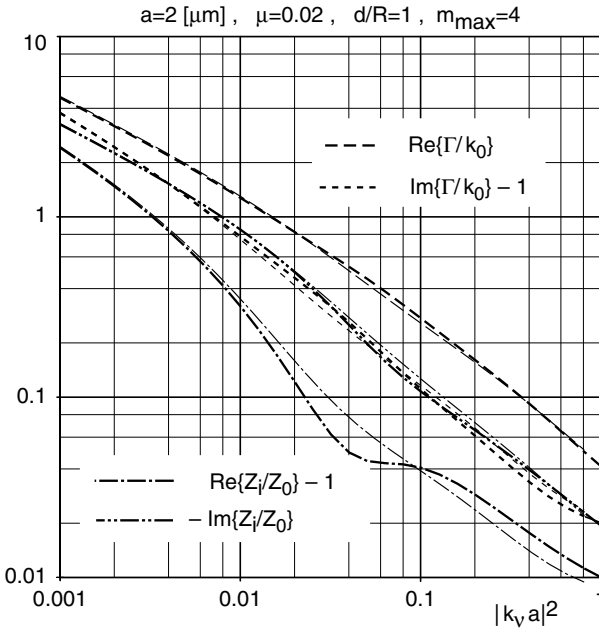
$$v_r(a, \varphi_i) = 0: \begin{cases} k_\rho a \cdot [A_{\rho n} H_n'^{(2)}(k_\rho a) - \dfrac{2\pi N}{k_\rho^2 - k_e^2} \, (-j)^n \, J_n'(k_\rho a) \cdot \displaystyle\sum_{m \geq 0} j^m \, B_{\rho mn} \cdot A_{\rho m}] \\[2ex] + k_\alpha a \cdot [A_{\alpha n} H_n'^{(2)}(k_\alpha a) - \dfrac{2\pi N}{k_\alpha^2 - k_e^2} \, (-j)^n \, J_n'(k_\alpha a) \cdot \displaystyle\sum_{m \geq 0} j^m \, B_{\alpha mn} \cdot A_{\alpha m}] \\[2ex] - n \cdot [A_{\nu n} H_n^{(2)}(k_\nu a) + \dfrac{2\pi N}{k_\nu^2 - k_e^2} \, (-j)^n \, J_n(k_\nu a) \cdot \displaystyle\sum_{m \geq 0} j^m \, B_{\nu mn} \cdot A_{\nu m}] \\[2ex] = -\delta_n \, (-j)^n \, k_e a \, J_n'(k_e a) \cdot A_E, \end{cases} \tag{8}$$

$$\frac{T(a, \varphi_i)}{T_0} = 0: \begin{cases} [A_{\rho n} H_n^{(2)}(k_\rho a) - \dfrac{2\pi N}{k_\rho^2 - k_e^2} \, (-j)^n \, J_n(k_e a) \cdot \displaystyle\sum_{m \geq 0} j^m B_{\rho mn} \cdot A_{\rho m}] \\[2ex] + \dfrac{\Theta_\alpha}{\Theta_\rho} \cdot [A_{\alpha n} H_n^{(2)}(k_\alpha a) - \dfrac{2\pi N}{k_\alpha^2 - k_e^2} \, (-j)^n \, J_n(k_\alpha a) \cdot \displaystyle\sum_{m \geq 0} j^m B_{\alpha mn} \cdot A_{\alpha m}] \\[2ex] = -\delta_n \, (-j)^n \, J_n(k_e a) \cdot A_E. \end{cases} \tag{9}$$

With a solution for the amplitudes $A_{\beta n}$, A_{vn} evaluate

$$\frac{\rho_{eff}}{\rho_0} = \frac{\left[r \cdot \left(\Phi_{Er1}(r) + \Phi_{\rho r1}(r) + \frac{\Pi_\alpha}{\Pi_\rho} \Phi_{\alpha r1}(r) \right) \right]_a^R}{[r \cdot (\Phi_{Er1}(r) + \Phi_{\rho r1}(r) + \Phi_{\alpha r1}(r) - \Psi_{zr1}(r))]_a^R},$$

$$\frac{C_{eff}}{C_0} = \frac{[\hat{\Phi}_{Er0}(r) + \hat{\Phi}_{\rho r0}(r) + \hat{\Phi}_{\alpha r0}(r)]_a^R}{\left[\frac{\rho_{eff}}{\rho_0} \frac{k_\rho^2}{k_e^2} \hat{\Phi}_{Er0}(r) + \hat{\Phi}_{\rho r0}(r) + \frac{\Pi_\alpha}{\Pi_\rho} \frac{k_\rho^2}{k_\alpha^2} \hat{\Phi}_{\alpha r0}(r) \right]_a^R}$$

(10)

with $[f(y)]_a^b = f(b) - f(a)$ and $\hat{\Phi}_\beta(r) = \int\limits^r k_\beta^2 r \cdot \Phi_\beta(r)\, dr.$

a=2 [µm] , µ=0.02 , d/R=1 , m_{max}=4

Comparison of the components of characteristic values in a transversal fibre bundle, evaluated iteratively for an effective propagating wave (thick lines, from this section), and with a propagating density wave (thin lines, from ⊳ Sect. G.8)

The evaluation must proceed iteratively because the equations from the boundary conditions contain (besides the unknown amplitudes) the unknown wave number k_e. Begin the iteration with an approximation $\Gamma = jk_e$ from ⊳ Sect. G.8; solve for a first approximation of $A_{\beta n}$, A_{vn}; insert into the expressions for ρ_{eff}, C_{eff}; evaluate the next approximation for the propagating wave from:

$$\frac{\Gamma}{k_0} = j\sqrt{\frac{\rho_{eff}}{\rho_0} \cdot \frac{C_{eff}}{C_0}} \quad ; \quad \frac{Z_e}{Z_0} = \sqrt{\frac{\rho_{eff}}{\rho_0} \bigg/ \frac{C_{eff}}{C_0}},$$

(11)

and resume the cycle of iteration. Apply in the evaluations, with the massivity μ:

$$\frac{a}{R} = \sqrt{\mu} \quad ; \quad \frac{2\pi N}{k_\beta^2 - k_e^2} = \frac{2\mu}{(k_\beta a)^2 - (k_e a)^2}. \tag{12}$$

The diagram above compares the components of the characteristic values from the present iterative evaluation (with an "effective" propagating wave) with values from ▶ *Sect. G.8* (with the density wave as the propagating wave). Up to $m_{max} = 4$ orders of scattering were used.

Notice that the theoretical curves of this section reproduce the humps of the experimental points in the figure from ▶ *Sect. G.4*.

The present method, although much more complicated numerically than the method of ▶ *Sect. G.8*, is well suited to evaluate particle velocity profiles around a fibre in a transversal fibre bundle.

$|k_v a|^2 = 1.024$, $\mu = 0.02$, $m_{max} = 8$
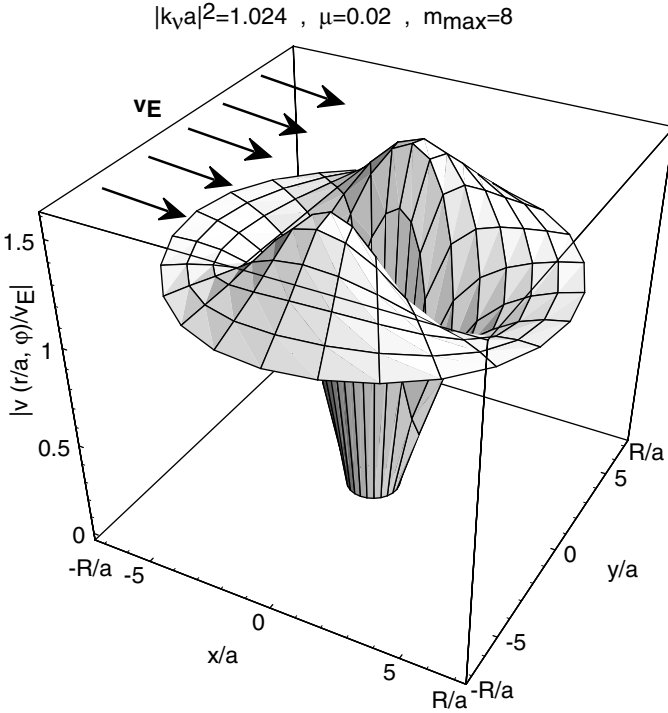
Profile of the magnitude of the total particle velocity around a fibre in a fibre bundle with transversal sound propagation

$|k_\nu a|^2 = 1.024$, $\mu = 0.02$, $m_{max} = 4$
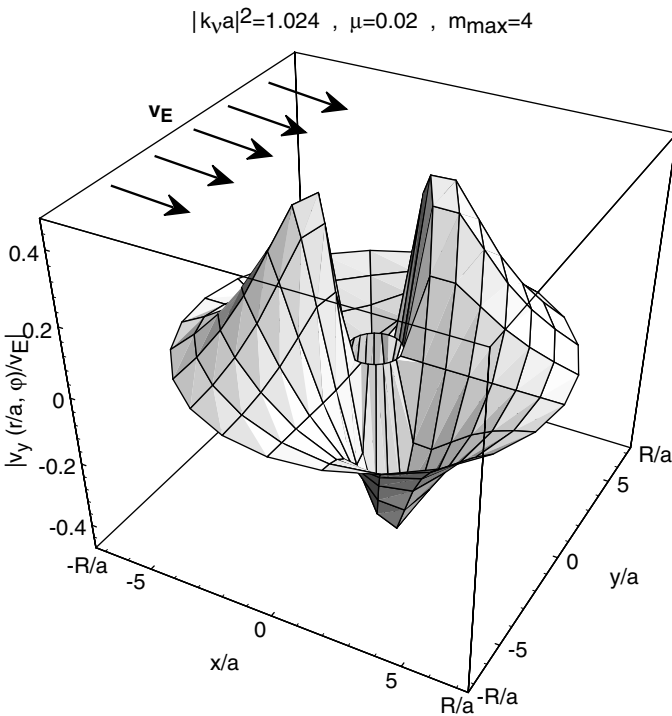
Profile of the real component of the transversal particle velocity around a fibre in a fibre bundle with transversal sound propagation

G.10   Biot's Theory of Porous Absorbers

▶ *See also:* Tolstoy (1992), a survey in Mechel (1995)

Whereas in other sections of this chapter the matrix of the porous material is assumed to be rigid, it may be elastic in Biot's theory. The consequence of this elasticity is the onset of additional wave types by the coupling between the matrix and the enclosed fluid in the pores. Biot's theory is not a "terminated" theory; he took some fundamental relations between flow and sound from the theory of circular capillaries, which was available at his time, instead of results from possibly better suited models which are now available. The price for the wider range of application of Biot's theory is a number of specially defined material parameters, for which Biot has given prescriptions on how to measure them.

Fundamental assumptions:

- The matrix is homogeneous and isotropic in scales which are larger than the scale of the pores.
- The pores are interconnected.
- The size of the pores is small compared to considered volume elements dV and small compared to the wavelength.

Fundamental equations:

Let $\vec{u}_s$ be the movement (elongation) of a solid, averaged over a volume element dV;

let $\vec{u}_f$ be the average movement of the fluid in dV.

Equations of motion:

$$\rho_{ss}\frac{\partial^2\vec{u}_s}{\partial t^2} + \rho_{sf}\frac{\partial^2\vec{u}_f}{\partial t^2} = P \cdot \text{grad div } \vec{u}_s + Q \cdot \text{grad div } \vec{u}_f$$

$$- N \cdot \text{rot rot } \vec{u}_s + bF(\omega) \cdot \left(\frac{\partial\vec{u}_f}{\partial t} - \frac{\partial\vec{u}_s}{\partial t}\right),$$
(1)

$$\rho_{ff}\frac{\partial^2\vec{u}_f}{\partial t^2} + \rho_{sf}\frac{\partial^2\vec{u}_s}{\partial t^2} = R \cdot \text{grad div } \vec{u}_f$$

$$+ Q \cdot \text{grad div } \vec{u}_s - bF(\omega) \cdot \left(\frac{\partial\vec{u}_f}{\partial t} - \frac{\partial\vec{u}_s}{\partial t}\right).$$
(2)

Strain-stress equations:

$$\tau_{ij}^s = [(P - 2N) \cdot \text{div } \vec{u}_s + Q \cdot \text{div } \vec{u}_f]\,\delta_{ij} + N \cdot \left(\frac{\partial u_{si}}{\partial x_j} + \frac{\partial u_{sj}}{\partial x_i}\right),$$
(3)

$$\tau_{ij}^f = -\sigma\,p\,\delta_{ij} = [R \cdot \text{div } \vec{u}_f + Q \cdot \text{div } \vec{u}_s]\,\delta_{ij},$$

where u_{si} are the components of $\vec{u}_s$ in the direction of the co-ordinate x_i; τ^s is the tension on the matrix absorber in a unit area; τ^f is the tension on the fluid in a unit area; i, j = 1, 2, 3 denote co-ordinates; τ_{33}^s is the x_3 component of the tension on the matrix acting on a surface normal to x_3; and τ_{13}^s denotes a shear tension in the x_1 direction on a surface normal to x_3. δ_{ij} is the Kronecker symbol. ρ_{mn} are effective mass densities if m = n; they are coupling coefficients between a solid and a fluid if m ≠ n. A, P, Q, R, N are elastic constants, introduced by Biot. A corresponds to the first Lamé constant of a material matrix, N to its second Lamé constant. In most cases P = A + 2N holds. Q evidently is a coupling coefficient between matrix and fluid; it determines also the coefficient R by the relation R = −Q · e/ε, where e = div $\vec{u}_s$ and ε = div $\vec{u}_f$ are the strains of the solid and the fluid, respectively. There are three coupling coefficients between solid and fluid in the equations: ρ_{sf}, $bF(\omega)$, and Q.

With σ = volume porosity of the porous material, the effective densities are:

$$\rho_{ss} = (1 - \sigma)\,\rho_s - \rho_{sf} \quad ; \quad \rho_{ff} = \sigma\,\rho_0 - \rho_{sf},$$
(4)

where ρ_s is the density of the (compact) solid and $\rho_0 = \rho_f$ is the density of the fluid. The coupling density ρ_{sf} describes the extra inertia of a relative motion between solid and fluid:

$$\rho_{sf} = -(\chi - 1)\,\sigma\,\rho_0.$$
(5)

The term χ represents the *tortuosity* of the pores in the material (it corresponds to the structure factor in older theories; see below for its determination); it is a pure form factor.

The term $bF(\omega)$ is a coupling factor of the viscous forces; it is associated with the relative velocity $\partial\vec{u}_f/\partial t - \partial\vec{u}_s/\partial t$ of fluid and solid. It is mainly determined by the flow resistivity Ξ of the material; it is frequency dependent, whereby the transition from an approximately parabolic flow profile at low frequencies into an approximately rectangular profile at high frequencies can be described. Biot has taken the quantity $bF(\omega)$ from the observation that the effective densities ρ_{eff} in flat and in circular capillaries have about the same frequency dependence, up to a "stretching" of the frequency axis with a factor c [see the sections on sound in capillaries in ▶ Ch. J, "Duct Acoustics"; see there also for the definition of $J_{1,0}(z)$]. Thus he took from circular capillaries (a = pore radius in the capillary model, $k_v = -j\sqrt{(\omega/\nu)}$, ν = kinematic viscosity):

$$b\,F(\omega) = -\frac{\sigma^2\Xi}{4}\ \frac{c\,k_v a \cdot J_{1,0}(c\,k_v a)}{1 - \dfrac{2}{c\,k_v a}\,J_{1,0}(c\,k_v a)}. \tag{6}$$

The equivalent radius a of the capillary for a given porous material can be taken from:

$$\Xi = \frac{8\eta}{a^2}\frac{\chi}{\sigma} \quad (\eta = \text{dynamic viscosity}), \tag{7}$$

where Ξ the measured flow resistivity, σ the porosity and χ the tortuosity. The matching factor c in the argument of $J_{1,0}(z)$ changes between c $=$ 1 for cylindrical pores and c $= (4/3)^{1/2}$ for flat pores; values for triangular and square pores have been evaluated.

A different method (from Johnson et al.) to determine $bF(\omega)$ is:

$$b\,F(\omega) = \sigma^2\Xi\ \left(1 + \frac{4j\,\chi^2\eta\rho_0\omega}{\Xi^2\Lambda^2\sigma^2}\right)^{1/2} \quad ; \quad \Lambda = c\left(\frac{8\eta\chi}{\Xi\sigma}\right)^{1/2}. \tag{8}$$

The coupling factor Q is called the *potential coupling* factor. It takes into account the fact that the pressure in the pores may change, even if div $\vec{u}_f = 0$ in the pores, by a dilatation of the matrix.

If only shear stresses act on the absorber, no dilatation takes place; the strain-stress equations reduce to:

$$\tau_{ij}^s = N\left[\frac{\partial u_{si}}{\partial x_j} + \frac{\partial u_{sj}}{\partial x_i}\right]; \tau_{ij}^f = 0, \tag{9}$$

thus N is the shear modulus of the matrix.

Suppose a sample of the porous material is coated with a thin, limp foil, allowing a connection between the inside and outside space, and exerts a static pressure P_s on the coated sample. Whereas the matrix may be deformed, the pressure in the pores remains constant.
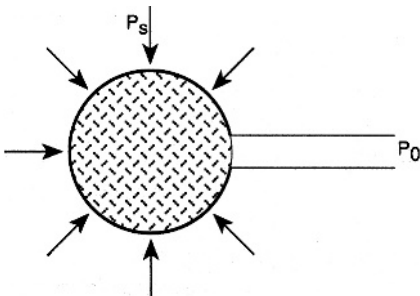
The strain-stress equations simplify to:

$$-P_s = \left(P - \frac{4}{3}N\right) \cdot \text{div } \vec{u}_s + Q \cdot \text{div } \vec{u}_f; \quad 0 = R \cdot \text{div } \vec{u}_f + Q \cdot \text{div } \vec{u}_s. \tag{10}$$

After elimination of $\vec{u}_f$:

$$K_b = P - \frac{4}{3}N - \frac{Q^2}{R}, \tag{11}$$

where $K_b = -P_s/\text{div } \vec{u}_s$ is the bulk compression modulus of the matrix. (12)

Suppose further that a material sample is subjected (in a tank) to a hydrostatic pressure p_f. The forces acting on the matrix and the pores are $(1 - \sigma) \cdot p_f$ and $\sigma \cdot p_f$, respectively. The strain-stress equations become:

$$-(1 - \sigma) p_f = \left(P - \frac{4}{3}N\right) \cdot \text{div } \vec{u}_s + Q \cdot \text{div } \vec{u}_f \ ; \quad -\sigma p_f = R \cdot \text{div } \vec{u}_f + Q \cdot \text{div } \vec{u}_s. \tag{13}$$

With K_s the compression modulus of the compact matrix material and K_f the compression modulus of the fluid in the pores, one gets:

$$P = \frac{(1 - \sigma)(1 - \sigma - K_b/K_s) K_s + (K_s/K_f) K_b}{1 - \sigma - K_b/K_s + \sigma K_s/K_f} + \frac{4}{3}N,$$

$$Q = \frac{(1 - \sigma - K_b/K_s) \sigma K_s}{1 - \sigma - K_b/K_s + \sigma K_s/K_f}, \tag{14}$$

$$R = \frac{\sigma^2 K_s}{1 - \sigma - K_b/K_s + \sigma K_s/K_f}.$$

In many materials $K_s \gg K_b$ and $K_s \gg K_f$; then the equations simplify to:

$$P = K_b + \frac{4}{3}N + \frac{(1 - \sigma)^2}{\sigma} K_f \quad ; \quad Q = (1 - \sigma) K_f \quad ; \quad R = \sigma K_f. \tag{15}$$

The compression modulus K_f of the fluid in the pores changes from isothermal compression at low frequencies (if the heat capacity and heat conduction of the matrix material are much larger than those of the fluid) to adiabatic compression at high frequencies. This transition is taken from the model of circular capillary pores (with the same fitting parameter c from above for other pore shapes):

$$K_f = \rho_0 c_0^2 / [1 + (\kappa - 1) J_{1,0}(c \, k_{\alpha 0} a)], \tag{16}$$

where a is the equivalent pore radius, κ is the adiabatic exponent, $k_{\alpha 0} = \kappa Pr \cdot k_v$, Pr is a Prandtl number, k_v is the viscous wave number, and $J_{1,0}(z)$ (see ► *Ch. J*, "Duct Acoustics").

Wave equations:

The solution of the fundamental equations in principle consists of a triple of two longitudinal compressional waves and a transversal shear wave. The strain fields $\vec{u}_s$, $\vec{u}_f$ in the solid and the fluid are described by scalar and vector potentials:

$$\vec{u}_s = \text{grad } \Phi + \text{rot } \vec{H} \quad ; \quad \vec{u}_f = \text{grad } \Psi + \text{rot } \vec{G}. \tag{17}$$

Insertion into the fundamental equations gives:

$$\rho_{ss} \frac{\partial^2 \Phi}{\partial t^2} + \rho_{sf} \frac{\partial^2 \Psi}{\partial t^2} = P \cdot \text{div grad } \Phi + Q \cdot \text{div grad } \Psi + bF(\omega) \cdot \left(\frac{\partial \psi}{\partial t} - \frac{\partial \Phi}{\partial t} \right),$$

$$\rho_{ff} \frac{\partial^2 \Psi}{\partial t^2} + \rho_{sf} \frac{\partial^2 \Phi}{\partial t^2} = R \cdot \text{div grad } \Psi + Q \cdot \text{div grad } \Phi - bF(\omega) \cdot \left(\frac{\partial \Psi}{\partial t} - \frac{\partial \Phi}{\partial t} \right)$$

(18)

and

$$\rho_{ss} \frac{\partial^2 \vec{H}}{\partial t^2} + \rho_{sf} \frac{\partial^2 \vec{G}}{\partial t^2} = N \cdot \text{grad div } \vec{H} + bF(\omega) \cdot \left(\frac{\partial \vec{G}}{\partial t} - \frac{\partial \vec{H}}{\partial t} \right),$$

$$\rho_{ff} \frac{\partial^2 \vec{G}}{\partial t^2} + \rho_{sf} \frac{\partial^2 \vec{H}}{\partial t^2} = -bF(\omega) \cdot \left(\frac{\partial \vec{G}}{\partial t} - \frac{\partial \vec{H}}{\partial t} \right).$$

(19)

With a time factor $e^{j\omega t}$ and the abbreviations:

$$\tilde{\rho}_{ss} = \rho_{ss} - j \frac{bF(\omega)}{\omega}; \quad \tilde{\rho}_{ff} = \rho_{ff} - j \frac{bF(\omega)}{\omega}; \quad \tilde{\rho}_{sf} = \rho_{sf} + j \frac{bF(\omega)}{\omega}; \quad \tilde{\chi} = \chi - j \frac{bF(\omega)}{\omega \sigma \rho_0}, \quad (20)$$

one gets:

$$-\omega^2 (\tilde{\rho}_{ss} \Phi + \tilde{\rho}_{sf} \Psi) = P \cdot \Delta \Phi + Q \cdot \Delta \Psi,$$

$$-\omega^2 (\tilde{\rho}_{ff} \Psi + \tilde{\rho}_{sf} \Phi) = R \cdot \Delta \Psi + Q \cdot \Delta \Phi.$$

(21)

Elimination of $\Delta \Psi$ yields:

$$\Psi = \frac{(PR - Q^2) \cdot \Delta \Phi + \omega^2 (\tilde{\rho}_{ss} R - \tilde{\rho}_{sf} Q) \cdot \Phi}{\omega^2 (\tilde{\rho}_{ff} Q - \tilde{\rho}_{sf} R)},$$

(22)

$$(PR - Q^2) \cdot \Delta^2 \Phi + \omega^2 (\tilde{\rho}_{ss} R + \tilde{\rho}_{ff} P - 2\tilde{\rho}_{sf} Q) \cdot \Delta \Phi + \omega^4 (\tilde{\rho}_{ss} \tilde{\rho}_{ff} - \tilde{\rho}_{sf}^2) \cdot \Phi = 0.$$

The last equation is formally interpreted as a product of two wave equations $(\Delta - k_1^2) \cdot (\Delta - k_2^2) \Phi = 0$ with a solution $\Phi = \Phi_1 + \Phi_2$ of which the sum terms obey: (23)

$$(\Delta - k_1^2) \Phi_1 = 0 \quad ; \quad (\Delta - k_2^2) \Phi_2 = 0,$$

$$k_{1,2}^2 = \frac{\omega^2}{2(PR - Q^2)} [(\tilde{\rho}_{ss} R + \tilde{\rho}_{ff} P - 2\tilde{\rho}_{sf} Q) \pm \sqrt{D}],$$

(24)

$$D = (\tilde{\rho}_{ss} R + \tilde{\rho}_{ff} P - 2\tilde{\rho}_{sf} Q)^2 - 4(PR - Q^2)(\tilde{\rho}_{ss} \tilde{\rho}_{ff} - \tilde{\rho}_{sf}^2).$$

There are two compressional waves $\Phi_{1,2}$ in the solid with characteristic wave numbers $k_{1,2}$.

The scalar potential Ψ for the sound wave in the fluid can be written as:

$$\Psi = \mu_1 \Phi_1 + \mu_2 \Phi_2,$$

$$\mu_{1,2} = \frac{\tilde{\rho}_{ss} R - \tilde{\rho}_{sf} Q - (PR - Q^2) k_{1,2}^2 / \omega^2}{\tilde{\rho}_{ff} Q - \tilde{\rho}_{sf} R}.$$

(25)

The vector potentials $\vec{G}$, $\vec{H}$ can be derived similarly. One finds:

$$\vec{G} = -\frac{\tilde{\rho}_{sf}}{\tilde{\rho}_{ff}} \cdot \vec{H} = \mu_3 \cdot \vec{H} \quad ; \quad \Delta\vec{H} - \frac{\omega^2}{N}\left(\frac{\tilde{\rho}_{ss}\tilde{\rho}_{ff} - \tilde{\rho}_{sf}^2}{\tilde{\rho}_{ff}}\right) \cdot \vec{H} = \left(\Delta - k_3^2\right)\vec{H} = 0,$$

$$k_3^2 = \frac{\omega^2}{N}\frac{\tilde{\rho}_{ss}\tilde{\rho}_{ff} - \tilde{\rho}_{sf}^2}{\tilde{\rho}_{ff}} \quad ; \quad \mu_3 = -\frac{\tilde{\rho}_{sf}}{\tilde{\rho}_{ff}}. \tag{26}$$

Special case: weak coupling, densities of solid and fluid very different

In many porous absorber materials the porosity is $\sigma \approx 1$, the tortuosity is $1 \leq \chi \leq 2$, the density of the solid material is $\tilde{\rho}_{ss} \gg \tilde{\rho}_{ff}$, and also $\tilde{\rho}_{ss} \gg \tilde{\rho}_{sf}$. Then BIOT's parameters simplify to:

$$P \approx K_b + \frac{4}{3}N; \quad Q \approx 0; \quad R \approx K_f, \tag{27}$$

the wave numbers of the compressional waves approximately become:

$$k_1^2 \approx \omega^2\left[\frac{\tilde{\rho}_{ss}}{P} - \frac{\tilde{\rho}_{ss}\tilde{\rho}_{ff} - \tilde{\rho}_{sf}^2}{R\tilde{\rho}_{ss}}\right] \quad ; \quad k_2^2 \approx \omega^2\left[\frac{\tilde{\rho}_{ff}}{R} - \frac{\tilde{\rho}_{sf}^2}{R\tilde{\rho}_{ss}}\right], \tag{28}$$

and the amplitude ratio of the shear wave to the compressional waves is:

$$\mu_1 \approx -\frac{P}{R}\left(\frac{\tilde{\rho}_{ff}}{\tilde{\rho}_{sf}} - \frac{\tilde{\rho}_{sf}}{\tilde{\rho}_{ss}}\right) \quad ; \quad \mu_2 \approx -\frac{\tilde{\rho}_{ss}}{\tilde{\rho}_{sf}} + \frac{P}{R}\left(\frac{\tilde{\rho}_{ff}}{\tilde{\rho}_{sf}} - \frac{\tilde{\rho}_{sf}}{\tilde{\rho}_{ss}}\right). \tag{29}$$

The condition for this weak coupling is satisfied at frequencies above $f = \sigma^2 \Xi / 2\pi(1 - \sigma)\rho_s$.

The effective densities are, under the mentioned conditions:

$$\tilde{\rho}_{ss} \approx (1 - \sigma)\rho_s - j\frac{bF(\omega)}{\omega} \quad ; \quad \tilde{\rho}_{ff} \approx \sigma\rho_0 - j\frac{bF(\omega)}{\omega} \quad ; \quad \tilde{\rho}_{sf} \approx j\frac{bF(\omega)}{\omega}. \tag{30}$$

One gets for not too high flow resistivities Ξ:

$$k_1^2 \approx \omega^2\left[\frac{\tilde{\rho}_{ss}}{P} + \frac{\tilde{\rho}_{sf}^2}{\tilde{\rho}_{ss}R - \tilde{\rho}_{ff}P}\right] \quad ; \quad k_2^2 \approx \omega^2\left[\frac{\tilde{\rho}_{ff}}{R} - \frac{\tilde{\rho}_{sf}^2}{\tilde{\rho}_{ss}R - \tilde{\rho}_{ff}P}\right]. \tag{31}$$

The amplitude ratios are then:

$$\mu_1 \approx \frac{\tilde{\rho}_{ss} - P k_1^2/\omega^2}{-\tilde{\rho}_{sf}} \approx \frac{P\tilde{\rho}_{sf}}{\tilde{\rho}_{ss}R - \tilde{\rho}_{ff}P},$$

$$\mu_2 \approx \frac{\tilde{\rho}_{ss} - P k_2^2/\omega^2}{-\tilde{\rho}_{sf}} \approx \frac{(\tilde{\rho}_{ss}R - \tilde{\rho}_{ff}P)^2 + PR\tilde{\rho}_{sf}}{(\tilde{\rho}_{ss}R - \tilde{\rho}_{ff}P)R\tilde{\rho}_{sf}}. \tag{32}$$

The wave number of the shear wave approximates the value for that wave in the evacuated matrix:

$$k_3^2 \approx \frac{\omega^2}{N}(1 - \sigma)\rho_s \quad ; \quad \mu_3 \approx 0. \tag{33}$$

Input impedance of a porous layer with rigid backing (as an example)

A plane wave is incident under a polar angle Θ on a plane layer of a porous material with thickness d. The graph below shows schematically the three excited waves in the layer.
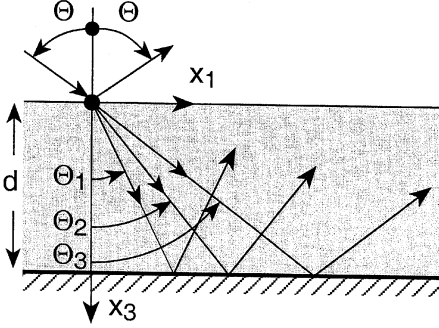
The three waves are formulated as three displacement potential functions; φ_3 is the not vanishing component of the vector potential $\vec{H}$ of the shear wave:

In forward direction:

$$\varphi_n = A_n \cdot e^{-jk_n(x_1 w_{n1} + x_3 w_{n3})}; \quad n = 1, \ 2, \ 3. \tag{34}$$

Waves reflected at the hard wall:

$$\psi_n = B_n \cdot e^{-jk_n(x_1 w_{n1} - x_3 w_{n3})}; \quad n = 1, \ 2, \ 3. \tag{35}$$

From Snell's law, where k_n are the Biot wave numbers:

$$k_0 \ \sin \Theta = w_{n1} k_n; \quad w_{n3} = \sqrt{1 - w_{n1}}. \tag{36}$$

The layer is in close contact with the hard wall at $x_3 = d$; thus

$$u_{s1}(x_1, d) = u_{s3}(x_1, d) = u_{f3}(x_1, d) = 0. \tag{37}$$

Special case of an open front side: i.e. no cover sheet on the absorber layer

Let p be the sound pressure and v_3 the particle velocity in the x_3 direction in front of the absorber; therefore (with the common factor in x_1 dropped and an unit amplitude of the incident wave supposed):

$$v_3 = \frac{\cos \Theta}{Z_0}(1 - R); \quad p = 1 + R, \tag{38}$$

where R is the reflection factor of the layer. Boundary conditions on the front side are:

$$v_3 = j\omega\left[(1 - \sigma)u_{s3} + \sigma u_{f3}\right] \ ; \quad -(1 - \sigma)p = \tau_{33}^s \ ; \quad -\sigma p = \tau_{33}^f. \tag{39}$$

The field formulations, when inserted into the boundary conditions at the back and front sides, give the following system of six equations:

$$u_{s1} = -jk_1w_{11}(A_1e^{-jk_1w_{13}d} + B_1e^{+jk_1w_{13}d})$$
$$-jk_2w_{21}(A_2e^{-jk_2w_{23}d} + B_2e^{+jk_2w_{23}d})$$
$$+jk_3w_{33}(A_3e^{-jk_3w_{33}d} - B_3e^{+jk_3w_{33}d}) = 0,$$

$$u_{s3} = -jk_1w_{13}(A_1e^{-jk_1w_{13}d} - B_1e^{+jk_1w_{13}d})$$
$$-jk_2w_{23}(A_2e^{-jk_2w_{23}d} - B_2e^{+jk_2w_{23}d})$$
$$-jk_3w_{31}(A_3e^{-jk_3w_{33}d} + B_3e^{+jk_3w_{33}d}) = 0,$$

$$u_{f3} = \mu_1[-jk_1w_{13}(A_1e^{-jk_1w_{13}d} - B_1e^{+jk_1w_{13}d})]$$
$$+ \mu_2[-jk_2w_{23}(A_2e^{-jk_2w_{23}d} - B_2e^{+jk_2w_{23}d})]$$
$$+ \mu_3[-jk_3w_{31}(A_3e^{-jk_3w_{33}d} + B_3e^{+jk_3w_{33}d})] = 0,$$

$$\tau_{33}^s = (P - 2N)\,\mathrm{div}\,\vec{u}_s + Q\,\mathrm{div}\,\vec{u}_f + 2N\frac{\partial u_{s3}}{\partial x_3}$$ (40)
$$= (P - 2N + \mu_1 Q)(-k_1^2(A_1 + B_1))$$
$$+ (P - 2N + \mu_2 Q)(-k_2^2(A_2 + B_2))$$
$$+ 2N\,[-k_1^2w_{13}^2(A_1 + B_1) - k_2^2w_{23}^2(A_2 + B_2) - k_3^2w_{31}w_{33}(A_3 - B_3)\,]$$
$$= -(1 - \sigma)p,$$

$$\tau_{33}^f = Q\,\mathrm{div}\,\vec{u}_s + R\,\mathrm{div}\,\vec{u}_f$$
$$= (Q + \mu_1 R)(-k_1^2w_{13}^2(A_1 + B_1))$$
$$+ (Q + \mu_2 R)(-k_2^2w_{23}^2(A_2 + B_2))$$
$$= -\sigma p,$$

$$\tau_{13}^s = N\left(\frac{\partial u_{s1}}{\partial x_3} + \frac{\partial u_{s3}}{\partial x_1}\right)$$
$$= N[-k_1^2w_{11}w_{13}(A_1 - B_1) - k_2^2w_{21}w_{23}(A_2 - B_2) - k_3^2(A_3 + B_3)] = 0.$$

Together with the relation for the reflection factor these equations comprise a system of seven equations for A_1, B_1, A_2, B_2, A_3, B_3 and R. After a numerical solution, the input impedance Z of the absorber layer can be evaluated from:

$$\frac{Z}{Z_0} = \frac{1}{\cos\Theta}\frac{1 + R}{1 - R}.$$ (41)

Special case of an adhesive foil or membrane on the front side

Let ρ be the surface mass density of the foil, S its bending stiffness, T its tension in the case of a membrane. Let P_1 be immediately in front of the absorber, P_2 a point on the surface of the absorber, and P_3 a point immediately behind the front side of the absorber. The equations of motion of the foil are:

$$-\omega^2\rho\,u_3(P_2) = \tau_{33}^s(P_3) + \tau_{33}^f(P_3) - \tau_{33}^f(P_1) + T\frac{\partial^2 u_3(P_2)}{\partial x_3^2},$$

$$-\omega^2\rho\,u_1(P_2) = \tau_{13}^s(P_3) + S\frac{\partial^2 u_1(P_2)}{\partial x_3^2}.$$ (42)

With $\tau_{33}^f(P_1) = -p$ these equations can be transformed into:

$$-\omega^2 \rho_2 \, u_1(P_2) = \tau_{13}^s(P_3)$$

$$-\omega^2 \rho_1 \, u_3(P_2) = \tau_{33}^s(P_3) + \tau_{33}^f(P_3) - \tau_{33}^f(P_1),$$

(43)

with

$$\rho_1 = \rho - T \, k_0^2 \sin^2 \Theta / \omega^2 \quad ; \quad \rho_2 = \rho - S \, k_0^2 \sin^2 \Theta / \omega^2.$$

(44)

The boundary conditions at the front side now become:

$$u_{s3}(P_3) = u_{f3}(P_3) = u_3(P_2) = u_3(P_1) \quad ; \quad u_{s1}(P_3) = u_1(P_2).$$

(45)

Together with the boundary conditions at the back side one has seven equations; $((u_i)_n$ is the component in the direction x_n of u_i):

$$(j\omega\rho_1 - Z) \cdot j\omega u_3(P_2) - \tau_{33}^s(P_3) - \tau_{33}^f(P_3) = 0,$$

$$-\omega^2 \rho_2 \cdot (u_1)_1(P_3) - \tau_{13}^s(P_3) = 0,$$

$$(u_1)_3(P_2) = (u_2)_3(P_2),$$

$$(u_1)_1 = 0; \quad (u_2)_3 = 0; \quad (u_1)_3 = 0 \quad \text{at} \quad x_3 = d,$$

$$Z = \frac{-\tau_{33}^f(P_1)}{j\omega \, u_3(P_1)}.$$

(46)

The numerical solution of the system of equations, after insertion of the field formulations, gives the amplitudes of the wave components and the input impedance Z.
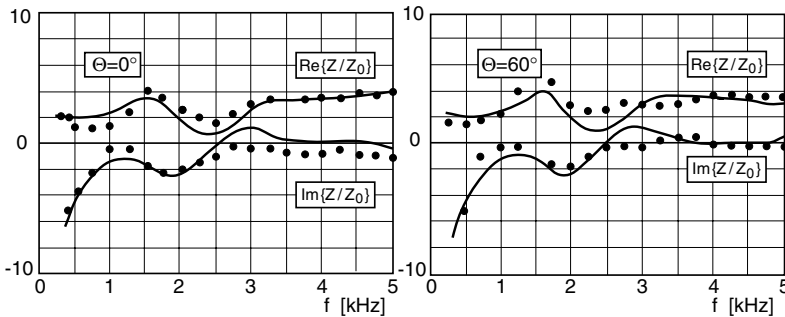
Measured (points) and evaluated (curves) components of the input impedance Z of an open layer of PU foam, d = 2 [cm] thick
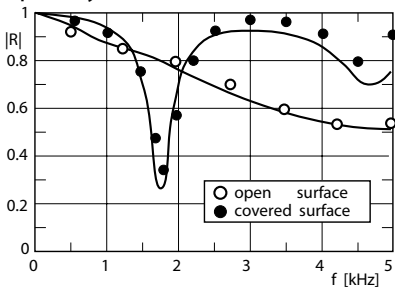
Measured (points) and evaluated (curves) magnitude of the reflection factor R of a d = 2 [cm] thick PU foam, once with open surface, once with a cover foil

G.11 Empirical Relations for Characteristic Values of Fibre Absorbers

▶ *See also:* Mechel (1995), Mechel/Grundmann (1982)

For a great number of glass fibre and mineral fibre absorber material from different producers and with a wide range of bulk densities the characteristic values, i.e. the propagation constant Γ_a and wave impedance Z_a, as well as the flow resistivity Ξ were carefully measured in Mechel/Grundmann (1982). The materials could be subdivided (from an acoustical point of view) into three product groups: glass fibre products, mineral fibre products (rockwool) and basalt wool products.

This section shows experimental values for the components of the normalised characteristic values $\Gamma_{an} = \Gamma_a/k_0 = \Gamma'_{an} + j \cdot \Gamma''_{an}$ and $Z_{an} = Z_{an}/Z_0 = Z'_{an} + j \cdot Z''_{an}$ over the "*absorber variable*" $E = \rho_0 f/\Xi$ (ρ_0 = density of air; f = frequency; Ξ = flow resistivity). It is advantageous (according to a proposal by Delany and Bazley) to plot Γ'_{an}, $\Gamma''_{an} - 1$, $Z'_{an} - 1, -Z''_{an}$ as functions of E, because the experimental data then group around simple curves, and to derive empirical relations for these quantities by regressions through the data.

The following table gives for the three product groups average values of (1) the fibre diameter d, (2) the distribution parameter Λ of a Poisson distribution of the diameters, to which the empirical distribution can be best matched, (3) the shot content (per weight, for shot with diameters > 100[µm]), and (4) the content of an organic binder (per weight).

**Table 1** Average technical data of fibre absorber materials

| Product group	Average fibre diameter dµm	Distribution parameter Λ(Δd = 1µm)	Shot content % (> 100µm)	Binder content %
Glass fibre	5.2	5.3	< 1	4.8
Basalt wool	3.9	4.0	32.4	1.0
Mineral fibre	4.0	2.8	27.1	2.1

The following diagrams show (for three product groups) experimental points, thick full curves from a floating average and thin dashed lines from the Delany and Bazley formula (see below).

Basalt wool — Γ'_{an}

Basalt wool — $\Gamma''_{an} - 1$

Basalt wool — $Z'_{an} - 1$

Basalt wool — $-Z''_{an}$
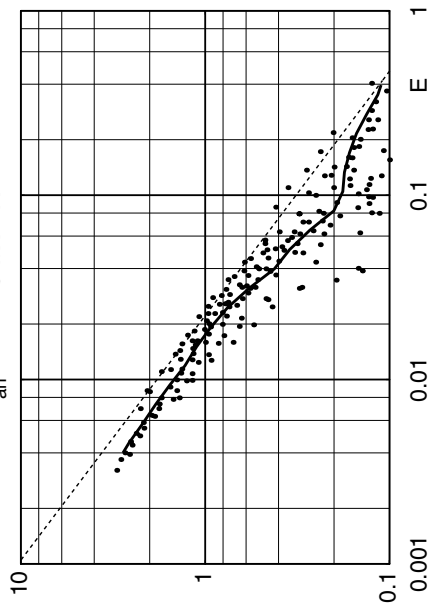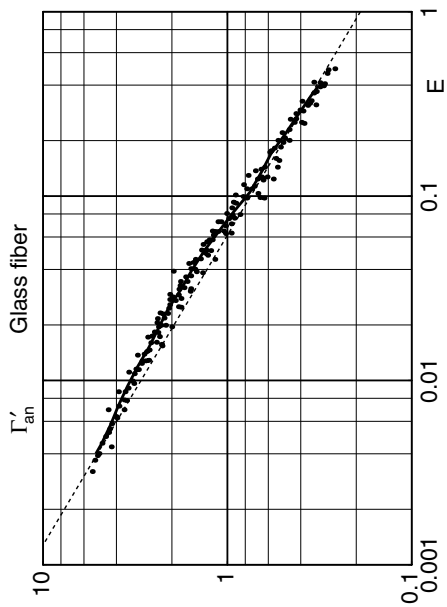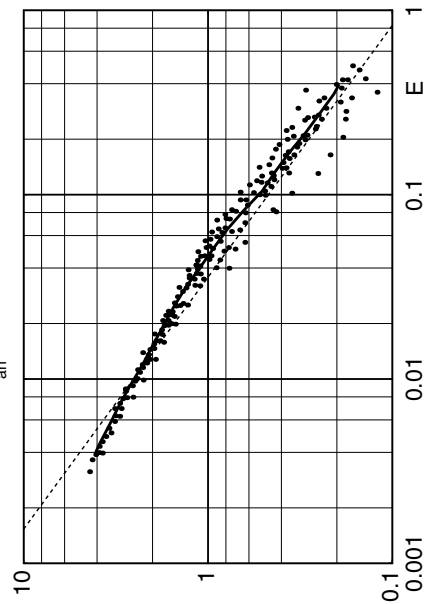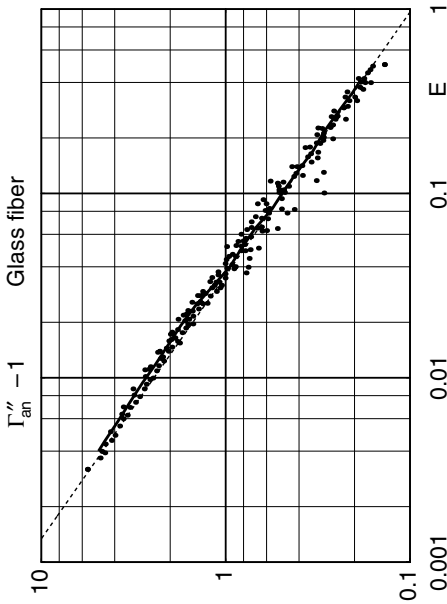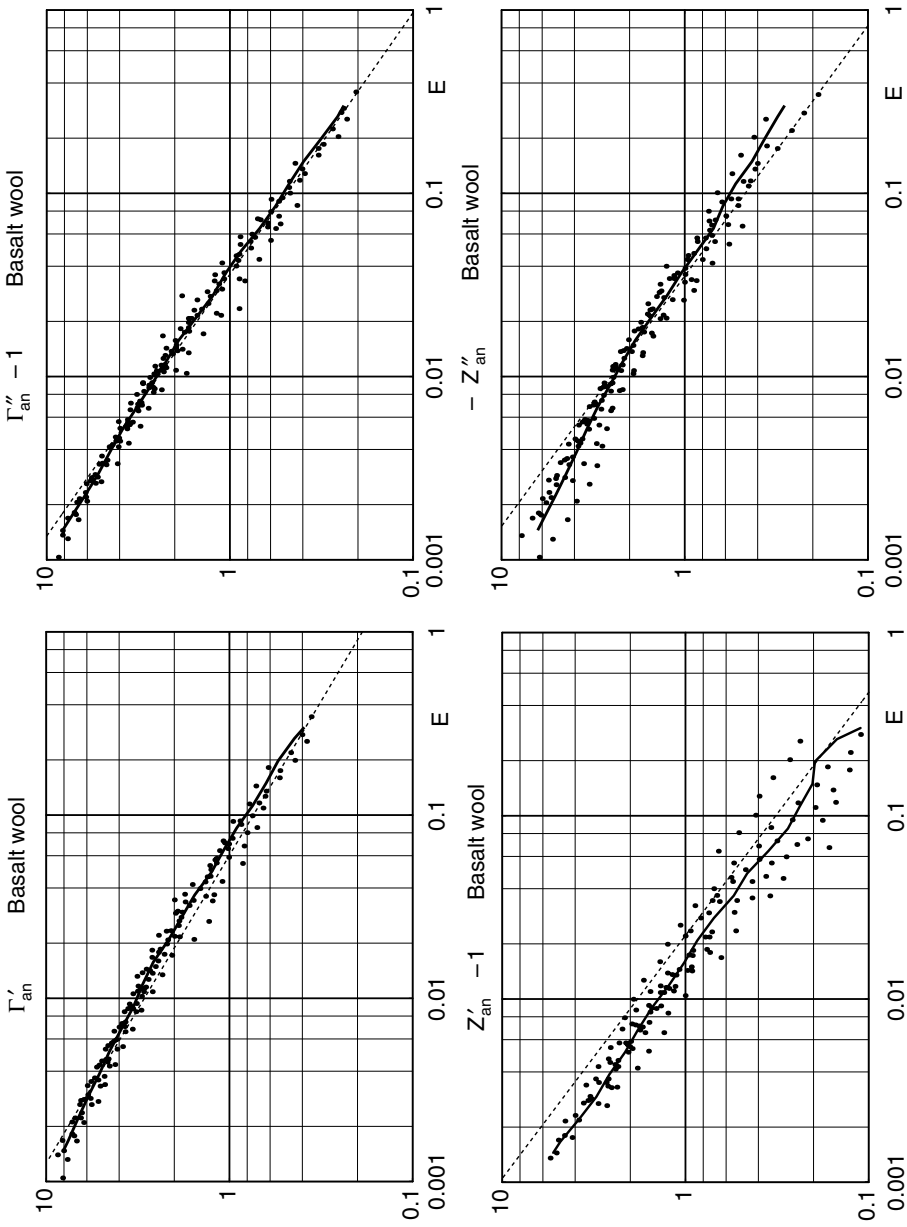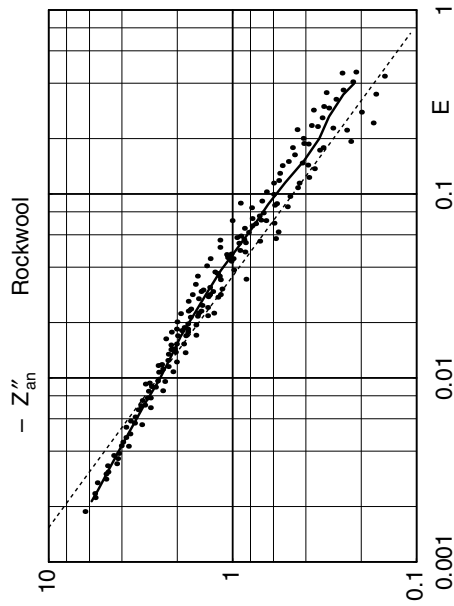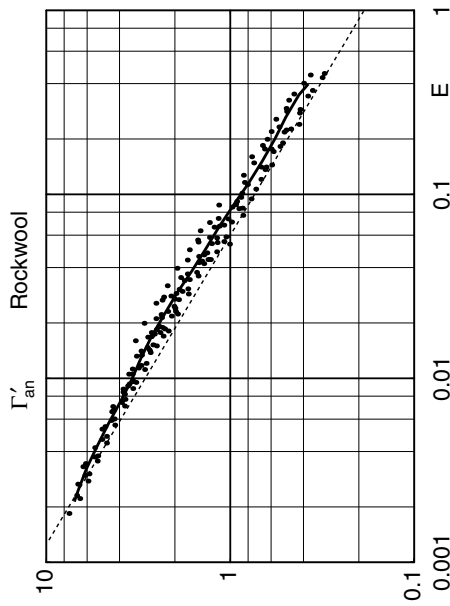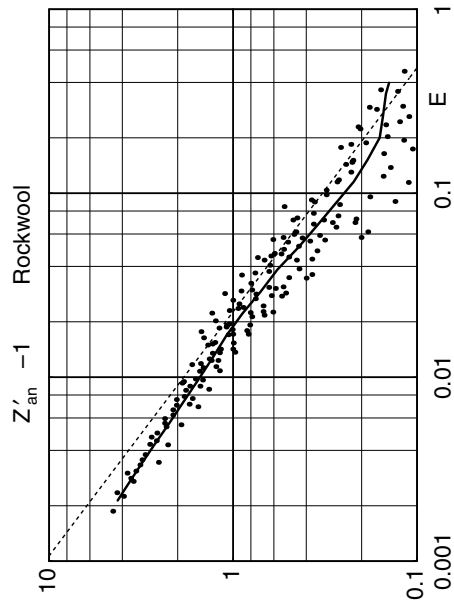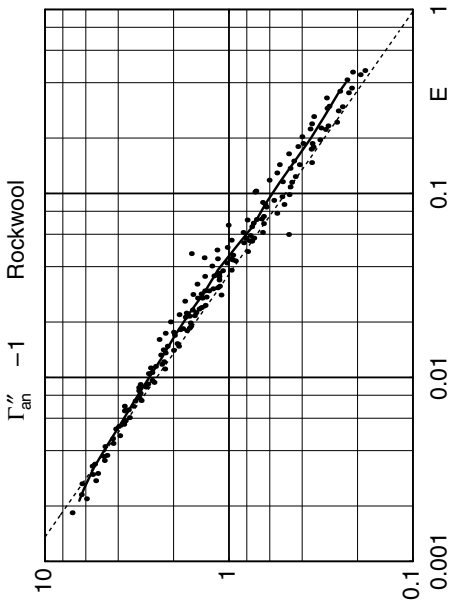
Delany and Bazley have represented their own experimental data for mineral fibre materials with the following formula, applicable at about $1 \le C \le 100$:

$$\Gamma_{an} = a' \cdot C^{\alpha'} + j \, (1 + a'' \cdot C^{\alpha''}) \quad ; \quad Z_{an} = 1 + b' \cdot C^{\beta'} - j \, b'' \cdot C^{\beta''} \tag{1}$$

using $C = 1/E = \Xi/(\rho_0 f)$ as an independent variable, and have given the following coefficients and exponents:

$$
\begin{aligned}
a' &= 0.189 \quad & \alpha' &= 0.595 \quad & a'' &= 0.0978 \quad & \alpha'' &= 0.700 \\
b' &= 0.0571 \quad & \beta' &= 0.754 \quad & b'' &= 0.087 \quad & \beta'' &= 0.732
\end{aligned}
\tag{2}
$$

The data by Mechel and Grundmann can be represented by:

$$CV = 10^{a_0 + a_1 \cdot \lg E + a_2 \cdot \lg^2 E + a_3 \cdot \lg^3 E} \quad ; \quad E = \frac{\rho_0 f}{\Xi} \quad ; \quad CV = \begin{cases} \Gamma'_{an} \\ \Gamma''_{an} - 1 \\ Z'_{an} - 1 \\ -Z''_{an} \end{cases} \tag{3}$$

in the range $0.003 \le E \le 0.4$, with the following coefficients (where rockwool and basalt wool products are combined to one group "mineral fibre"):

Table 2 Coefficients for relation (3)

CV	a_0 Mineral fibre Glass fibre	a_1 Mineral fibre Glass fibre	a_2 Mineral fibre Glass fibre	a_3 Mineral fibre Glass fibre
Γ'_{an}	−0.667583 −0.746924	−0.543980 −0.596783	0.0821882 0.107691	0.0278769 0.0435205
$\Gamma''_{an} - 1$	−0.886917 −0.937607	−0.528191 −0.474466	0.126739 0.210413	0.0321370 0.0524205
$Z'_{an} - 1$	−1.02007 −0.75754	−0.141648 0.814704	0.377471 1.12108	0.075733 0.239315
$-Z''_{an}$	−0.893386 −1.03401	−0.597382 −0.747567	0.0769774 0.0663115	0.0271011 0.0391343

The coefficients were determined for each component CV separately; thus the characteristic values are not analytic functions, which they should be for some applications. Therefore regressions were made with complex Γ_{an}, Z_{an}. They have the following form:

$$\left.\begin{aligned} \Gamma_{an} \\ Z_{an} \end{aligned}\right\} = \frac{\beta_{-1}}{E} + \frac{\beta_{-1/2}}{\sqrt{E}} + \beta_0 + \beta_{1/2}\sqrt{E} + \beta_1 E + \beta_{3/2}\sqrt{E^3} \tag{4}$$

with the coefficients (the last term with $\beta_{3/2}$ is only used with mineral fibre products):

Table 3 Coefficients for relations (4)

Coefficients	Γ_{an} Mineral fibre / Glass fibre		Z_{an} Mineral fiber / Glass fiber	
β_{-1}	$-0.00355757 - j\ 0.0000164897$ $-0.00451836 + j\ 0.000541333$		$0.0026786 + j\ 0.00385761$ $-0.00171387 + j\ 0.00119489$	
$\beta_{-1/2}$	$0.421329 + j\ 0.342011$ $0.421987 + j\ 0.376270$		$0.135298 - j\ 0.394160$ $0.283876 - j\ 0.292168$	
β_0	$-0.507733 + j\ 0.086655$ $-0.383809 - j\ 0.353780$		$0.946702 + j\ 1.47653$ $-0.463860 + j\ 0.188081$	
$\beta_{1/2}$	$-0.142339 + j\ 1.25986$ $-0.610867 + j\ 2.59922$		$-1.45202 - j\ 4.56233$ $3.12736 + j\ 0.941600$	
β_1	$1.29048 - j\ 0.0820811$ $1.13341 - j\ 1.74819$		$4.03171 + j\ 7.56031$ $-2.10920 - j\ 1.32398$	
$\beta_{3/2}$	$-0.771857 - j\ 0.668050$ 0		$-2.86993 - j\ 4.90437$ 0	

The regression is good in the "range of definition" $0.003 \leq E \leq 0.4$, but, as with all regressions, the errors become large if this range is exceeded.

G.12 Characteristic Values from Theoretical Models Fitted to Experimental Data

Simple numerical regressions through experimental data may return nonsense results if the range of definition of the regression is exceeded. For example, the original Delany and Bazley formula woud give a negative real part of the input impedance of a porous layer for low frequencies and/or high flow resistivity values. Some extension beyond that range is possible if theoretical models for porous materials are matched to experimental data by suitably fitting the parameters of the model theory because physical aspects can be taken into account when the parameters are fitted. The model theory must be simple enough for doing that.

The independent variable is $E = \rho_0 f / \Xi$
(ρ_0 = density of air, f = frequency, Ξ = flow resistivity)

Theory of the quasi-homogeneous material fitted to experimental data (⊙ *Sect. G.2*)

The characteristic values are evaluated from:

$$\Gamma_{an} = \frac{\Gamma}{k_0} = j\sqrt{\frac{\rho_{eff}}{\rho_0} \cdot \frac{C_{eff}}{C_0}} \quad ; \quad Z_{an} = \frac{Z_a}{Z_0} = \frac{1}{\sigma}\sqrt{\frac{\rho_{eff}}{\rho_0} \Big/ \frac{C_{eff}}{C_0}},$$

$$\frac{\rho_{eff}}{\rho_0} = \chi - j\frac{\sigma \cdot g(E)}{2\pi E} \quad ; \quad \frac{C_{eff}}{C_0} = \frac{\kappa + \alpha_1 \cdot j\,E/E_0}{1 + j\,E/E_0}, \tag{1}$$

$$g(E) = \gamma_0 + \gamma_1\ E + \gamma_2\ E^2$$

with fitted parameters for three product groups; $\sigma = 1 - \mu$ = porosity:

Table 1 Coefficients for the relations (1)

Parameters	Glass fibre	Basalt wool	Rockwool
χ	1.3	1.3	1.3
μ	0.02	0.02	0.02
κ	$1.40 + 0.15\ j$	$1.40 + 0.10\ j$	$1.40 + 0.15\ j$
α_1	1	1.1	1.1
E_0	0.125	0.10 (0.07 for Z_{an})	0.125
γ_0	1.09872	0.976206	1.12140
γ_1	0.333239	2.18474	1.49953
γ_2	1.62642	−1.26275	0.468552

The next diagram shows, as an example, the normalised propagation constant in glass fibre materials; the points are floating averages over experimental data, the thick solid lines come from the fitted theory, while the thin dashed curves belong to the original theory.
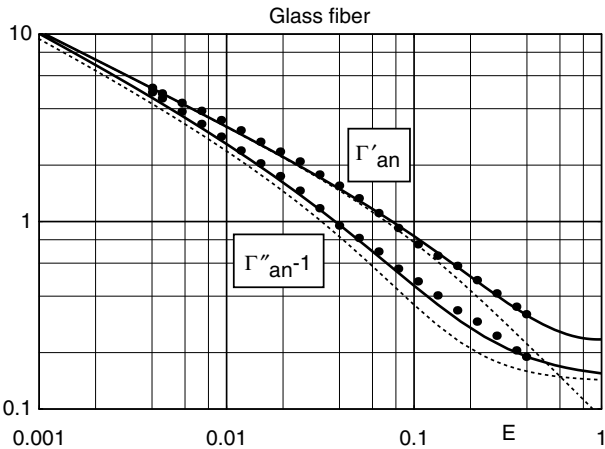
Components of the normalised propagation constant in glass fibre materials; points: floating average of experimental data, thick lines: fitted theory, thin lines: original theory

Fitted model of flat capillaries (❯ Sect. G.4)

The characteristic values are evaluated from:

$$\frac{\Gamma}{k_0} = \Gamma_{an} = j\sqrt{\frac{\rho_{eff}}{\rho_0} \cdot \frac{C_{eff}}{C_0}} \qquad ; \qquad \frac{Z_a}{Z_0} = Z_{an} = \frac{1}{\sigma}\sqrt{\frac{\rho_{eff}}{\rho_0} \Big/ \frac{C_{eff}}{C_0}},$$

$$\frac{\rho_{eff}}{\rho_0} = \frac{1}{1 - \dfrac{\tan\sqrt{-6\pi j\ a_1\ E}}{\sqrt{-6\pi j\ a_1\ E}}} \qquad ; \qquad \frac{C_{eff}}{C_0} = 1 + (\kappa - 1)\ \frac{\tan\sqrt{-6\pi j\ \kappa\ Pr\ a_2\ E}}{\sqrt{-6\pi j\ \kappa\ Pr\ a_2\ E}}, \qquad (2)$$

where Pr is a Prandtl number and $\sigma = 1 - \mu$ is the porosity and fitted parameters for three product groups:

Table 2 Coefficients for relations (2)

Material	Char. Value	μ	κ	a_1	a_2
Glass fibre	Γ_{an}	–	1.60 + 0.1 j	1	1
	Z_{an}	0.05	1.40 + 0.1 j	1	1.5
Basalt wool	Γ_{an}	–	1.40 + 0.15 j	1	1
	Z_{an}	0.05	1.40 + 0.1 j	0.9	1.7
Rockwool	Γ_{an}	–	1.70 + 0.1 j	1	0.6
	Z_{an}	0.05	1.40 + 0.1 j	0.9	1.7

The diagrams show the characteristic values for rockwool fibre materials (points: from floating averages over experimental data; curves: from fitted capillary model).

Rockwool
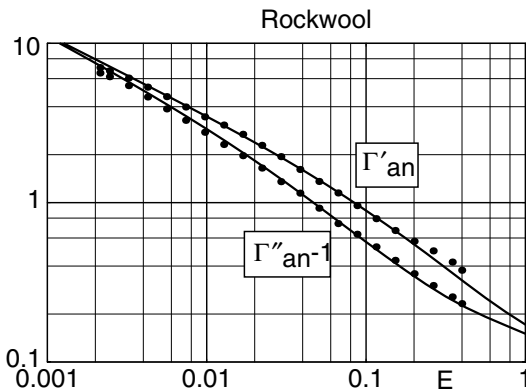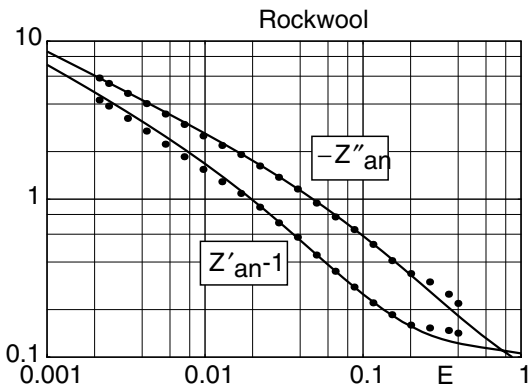
References

Mechel, F.P., Grundmann, R.: Akustische Kennwerte von Faserabsorbern, Vol. I, Bericht BS 85/83 (1983); Materialdaten, Vol. II, Bericht BS 75/82 (1982), Berichte des Fraunhofer-Instituts für Bauphysik, Stuttgart

Mechel, F.P.: Schallabsorber, Vol. II, Hirzel, Stuttgart (1995)

Tolstoy, I. (ed.): Acoustics, Elasticity, and Thermodynamics of Porous Media; Twenty-one Papers by M.A. Biot, Acoustical Society of America, American Institute of Physics, Melville, NY (1992)